# The effect of soy protein on adipocyte differentiation and lipid accumulation

By

Himali Silva

A thesis submitted to the Faculty of Graduate and Postdoctoral Affairs
In partial fulfillment of the requirements for the degree of

Master of Science

In

Biology

Carleton University

Ottawa, Ontario

**ABSTRACT**

Nutrition research is involved in combatting the obesity pandemic. Soy consumption is linked to a reduction of abdominal fat in rats. Currently, the bioactive soy protein subunit(s) and related molecular mechanism(s) associated with this effect remain unclear. This report examined the effect of soy glycinin and β-conglycinin on lipid accumulation and adipogenesis in rat adipose tissue and cultured mouse adipocytes. Mouse 3T3-L1 cells were differentiated in the presence of protein hydrolysates from Harovinton (conventional) and glycinin/β-conglycinin knockout strains. Sprague-Dawley rats (8 males, 8 females/group) were fed high-fat diets containing either 20% casein or 20% soy protein concentrates for 8 weeks. Harovinton increased lipid droplet size in 3T3-L1 cells ($p<0.01$) and increased mRNA ($p<0.03$) and protein levels ($p<0.001$) of peroxisome proliferator-activated receptor (PPARγ) in adipose tissue in female rats compared to casein control. This study showed that soy storage proteins may contribute to the maintenance of healthy white adipose tissue.

**ACKNOWLEDGEMENTS**

Firstly, I would like thank God for providing me with this incredible opportunity and for strengthening me throughout this journey.

I would like to sincerely thank my supervisors Dr. Steve Gleddie, Dr. Chaowu Xiao, and Dr. William Willmore for the privilege of working on this project. My time as a graduate student has been extremely rewarding, and I wish to express my gratitude for your guidance throughout this experience. I would also like to thank Dr. Douglas Johnson for serving on my committee and for providing valuable insight during the writing process.

My project would not have been successful without the support of my lab mates. In particular, I would like to thank Christine Gagnon, Carla Wood, Anne Hermans, Dr. Tri Vuong, and Dr. Cynthia Chatterjee for sharing your technical expertise and for dedicating time to helping me trouble-shoot the different aspects of my project. I am truly blessed by your kindness and friendship.

Additionally, I would like to acknowledge Dr. Syed Aziz, Kamla Kapal, and Anne Johnston for generously providing me with access to your laboratories during my project.

Finally, I would like to thank my family for your continued insight and support during this adventure.

**TABLE OF CONTENTS**

**LIST OF FIGURES**

**LIST OF TABLES**

**LIST OF ABBREVIATIONS**

| | |
|---|---|
| AMPK | 5' adenosine monophosphate- activated protein kinase α |
| B2m, *b2m* | Beta-2 microglobulin |
| cAMP | Cyclic adenosine monophosphate |
| cDNA | Complementary DNA |
| *c/ebpα* | CCAAT/enhancer-binding protein alpha gene |
| ddPCR | Digital drop polymerase chain reaction |
| DMSO | Dimethyl sulfoxide |
| *e2f/dp* | Transcription factor E2F/DP |
| ER/Erβ | Estrogen receptor/estrogen receptor β |
| FBS | Fetal bovine serum |
| FDA | US Food and Drug Administration |
| HDL | High-density lipoprotein |
| ISF | Isoflavone |
| Ldha, *ldha* | Lactate dehydrogenase A |
| LDL | Low-density lipoprotein |
| LPL | Lipoprotein lipase |
| NCS | Newborn calf serum |
| PBS | Phosphate-buffered saline |
| PCR | Polymerase chain reaction |
| PI3K | Phosphoinoside-3-kinase |
| PPARγ, *pparγ* | Peroxisome proliferator- activated receptor γ |

| | |
|---|---|
| PPRE | Peroxisome proliferator response element |
| SPI | Commercial soy protein isolate |
| TBST | Tris-buffered saline with 0.1% Tween-20 |
| THIF | 6,7,4'-trihydroxyisoflavone |
| UCP-1, *ucp-1* | Uncoupling protein 1 |
| *wnt-1* | Wingless-type MMTV integration site |

# 1 CHAPTER: INTRODUCTION

Obesity is defined as an excess accumulation in adipose tissue within the body and is quantified by a body mass index in excess of 30 (Shields, Gorber, & Tremblay, 2008; Tordjman, Guerre-Millo, & Clement, 2008). Excessive abdominal fat is often associated with cardiovascular disease, non-alcoholic fatty liver disease, Type II diabetes, osteoarthritis, and various forms of cancer (Janssen, 2013). In 2012, it was estimated that approximately 6.2 million Canadians were obese (Navaleen & Janz, 2014). Consequently, the obese population places a substantial burden on the healthcare system; in 2006, $3.9 billion of direct medical costs were spent on the obese population in Canada (Janssen, 2013). Obesity management has thus become a primary focus for both industry and health research.

With the population becoming more overweight and obese with each passing year, demand for weight management products and resources has risen substantially. Gyms, with frequent promotions and a wide variety of exercise classes, have become staples in most neighbourhoods, and an assortment of diet supplements, "natural" cleansing regimes, and "superfoods" grace the supermarket shelves. The term "superfood" is often used to describe a food whose vitamin, carbohydrate, protein, lipid, or mineral content has captured the interest of the weight management industry. It is important to note, however, that although such foods gain incredible popularity, their roles in weight loss or weight management are not always scientifically supported. The pursuit of novel superfoods led to

South East Asia, where, historically, populations favoured leaner physiques. It was speculated that the low prevalence of obesity in these countries was due to the traditional soy-based diets, which sparked an interest for the oilseed in the weight loss industry. Over the past few decades, soy (*Glycine max*) has become one of the leading superfoods in the North American market. One of the oilseed's primary advantages is its protein content. Soy contains all nine essential amino acids, making it comparable to meat protein and a viable vegetarian alternative (Friedman and Brandon, 2001). Moreover, studies show that increasing protein consumption increases satiety, thus making soy a much more attractive food option for those concerned with weight loss (Baba, et. al., 1999; Weigle, et al., 2005). In 1999, the US FDA approved a food labeling health claim linking soy protein consumption with decreased blood cholesterol levels thereby reducing the risk of coronary heart disease (US Food and Drug Administration, 2014). This official federal bulletin sparked keen interest in the North American population, and the subsequent demand for this new superfood led to the introduction of a plethora of soy products in the food industry, spurring agricultural changes as well. Over the next few years, research in soy linked seed consumption with prevention and/or treatment of several diseases, such as breast and prostate cancer, non-alcoholic fatty liver disease, and obesity, which further contributed to the growing popularity of soy (Friedman & Brandon, 2001; Janssen, 2013). Currently, soy is one of the highest value crops in Canada, with approximately 6 million metric tons of soybeans produced in 2014 (Soy Canada, 2014). While most of the Canadian soy crop is used

for animal feed production, soya has still become noteworthy for Canadian weight loss and commercial health industries as well as for Canadian health research.

Although the United States released their first claim in 1999, Canada was much more reluctant to make a formal statement due to the inconsistencies in soy research. It was only in late 2014 that Health Canada proposed a claim supporting the cholesterol-lowering effects of soy. A meta-analysis of international studies was performed that highlighted a soy-mediated decrease in high-density lipoprotein (HDL) cholesterol and blood triglyceride levels, and in March 2015, Health Canada published a health claim stating that a daily intake of 25g of soy protein does indeed reduce total cholesterol (Health Canada, 2015).

In this report, the hypolipidemic effect of soy were considered, with specific focus being directed to the effects of soy on adipose tissue. In a normal individual, excess dietary carbohydrates and lipids are converted to triglycerides and stored in adipose tissue; however, chronic high calorie diets impair proper triglyceride storage (Unger & Orci, 2000). Thus, other body tissues, including skeletal muscle, blood vessels, and hepatic tissue, become used as lipid storage sites (Lessard & Tchernof, 2012). Ectopic fat deposition results in excess cellular fatty acyl- CoA, which is thought to impede other metabolic pathways and leads to cellular apoptosis (Unger, 2002). Additionally, free fatty acids and triglycerides that adhere to blood vessels restrict blood flow and causes vascular cell apoptosis (Kavurma, Bhindi, Lowe, Chesterman, & Khachigan, 2005). Further implications of obesity on adipose tissue are discussed in Section 1.2. Thus, identification of a method of

restoring adipose tissue to proper functioning is paramount for preventing a wide variety of diseases. Soy protein was considered as a candidate for prompting adipose tissue development and improving its functioning.

## 1.1 Soy

For centuries, traditional Asian diets, such as Japanese and Korean diets, have prepared and consumed soy in a variety of different forms. While seeds may be consumed whole, in both the mature and immature state, they may also be soaked, heated, and pressed to produce soy milk or further coagulated to form tofu. Soy sauce is produced through the fermentation of soybeans with roasted grains, salt and yeast or mold. Textured soy protein is formed by pressing soy flour until it adopts the taste and texture of meat (Villares, Rostagno, Garica-Lafuentes, & Martinez, 2009). Soy products have also been incorporated into the North American food industry. Soy protein is often isolated and added as a fortifying agent to different commercial foods, such as wheat flour, to create more balanced food options. Since 20-30% of total soybean composition is attributed to lipids, most being unsaturated fats, soybean oil is now a highly favoured consumable (Alezandro, Granato, Lajolo, & Genovese, 2011). Additionally, soy lecithin, which is composed of phosphadidylcholine and various fatty acids including stearic and palmitic acid, is frequently used as an emulsifier and anti-spattering agent in food production (Oke, Jacob, & Paliya, 2010). Thus, soy products have become widely accepted in North America.

Analysis of soybean composition resulted in the identification of isoflavones and protein as the major functional components responsible for the proposed health benefits; they will be further discussed in Sections 1.1.1 and 1.1.2, respectively.

### 1.1.1 Soy isoflavones

Isoflavones are heterocyclic phenols found in various beans and oilseeds, including kidney beans, lentils, and chickpeas. In comparison with these other foods, soybeans contain the largest percentage of isoflavones, with concentrations ranging from 0.1 to 3mg per gram of soy protein (Vitale, Piazza, Melilli, Drago, & Salomone, 2012); the main types of isoflavones found in soy are genistein and daidzein (Seo et al., 2013). These plant-derived compounds are frequently referred to as phytoestrogens because they mimic the structure of estrogen and bind estrogen receptor α (ERα) and β (ERβ) (Vincent & Fitzpatrick, 2000). This property has been studied in detail for breast cancer and menopausal research. Soy isoflavone consumption has been shown to decrease menopausal hot flashes and reduce blood cholesterol levels in menopausal women (Vitale et al., 2012); however, many other areas of research remain inconclusive. Consumption of phytoestrogens does not appear to protect against menopausal osteoporosis and may stimulate cancer propagation in certain situations (Lagari & Levis, 2013; Yang, Belosay, Hartman, Song, Zhang, Wang, et al., 2015).

Of particular interest to this report is the phytoestrogenic impact on adipogenesis. Genistein and daidzein have been shown to mediate adipogenic processes in both skeletal muscle and adipose tissue. Genistein was shown to

decrease triglyceride accumulation in skeletal muscle through the up-regulation of AMPK, thus increasing fatty acid oxidation and thermogenesis (Palacios-Gonzalez et al., 2013). Seo et al. (2013) assessed the effect of 6,7,4'-trihydroxyisoflavone (THIF), a derivative of daidzein, on adipocyte differentiation in 3T3-L1 preadiopocytes. It was determined that THIF out-competed ATP to bind the adipogenic protein PI3K, and inhibited enzyme activity, thereby halting adipogenesis. Much research has already looked at the impact of isoflavones on obesity, but further research revealed that soy peptides may also directly affect adipogenesis.

### 1.1.2 Soy protein

Soybeans are considered a high-protein oilseed; depending on the variety, protein accounts for 35-56% of total soybean composition (Friedman & Brandon, 2001; Valasquez & Bhathena, 2007). Soy protein is labelled as a complete protein source, meaning they contain all nine essential amino acids, and is considered a good alternative to animal protein. Amino acid composition of the soy variety used in this project is found in Table 2. Soy protein isolate (SPI) have up to 92% of the nutritional value of milk protein, nutritional value being measured by the digestibility and levels of nitrogen absorption in the body (Mariotti, Mahe, Benamouzig, Luengo, Dare, Gudichon, et al., 1999). Consequently, casein, one of the most abundant proteins found in milk, often serves as a control when considering soy protein relative to animal protein.

**Table 2.** Amino acid (AA) composition and protein contents (grams of amino acids per kilogram of total protein; mean ± SEM) of Harovinton. Data modified from Zarkadas et al. (2007). Permission obtained from Elsevier.

| | Harovinton |
|---|---|
| Aspartic acid | 117.45 ± 0.95 |
| Threonine | 44.77 ± 1.77 |
| Serine | 47.67 ± 0.40 |
| Glutamic acid | 192.66 ± 1.62 |
| Proline | 54.19 ± 0.90[a] |
| Glycine | 37.82 ± 0.33 |
| Alanine | 40.29 ± 0.19 |
| Cysteine | 22.86 ± 0.73 |
| Valine | 51.82 ±0.47 |
| Methionine | 18.81 ± 0.71 |
| Isoleucine | 48.00 ± 0.6 |
| Leucine | 73.91 ± 0.36 |
| Tyrosine | 39.08 ± 0.30 |
| Phenylalanine | 52.20 ± 0.39 |
| Histidine | 27.74 ± 0.52 |
| Lysine | 63.96 ± 0.41 |
| Arginine | 77.95 ± 0.97 |
| Tryptophan | 13.07 ± 0.16 |
| Ammonia | 15.81 ± 0.56 |
| Ash μg/nmol | 0.114496 |
| Total protein g/kg of dry matter | 359.75 ± 3.39 |

It is important to note, however, that although soy and animal protein are frequently compared, there are some differences between the two. Proportions of lysine and methionine are lower in soybeans than in milk protein, and soy processing techniques have shown to further reduce bioavailability of these and other amino acids (Friedman & Brandon, 2001). For example, the acid spinning process to create soy-based meat alternatives results in the use of lysine for the synthesis of lysoalanine, an amino acid derivative with no nutritional benefits (Dosako, 1979). Despite these differences in amino acid composition, soy protein remains a viable alternative to animal protein. Of the total amount of soy protein, 80% comprises the storage proteins glycinin and β-conglycinin. In seeds, storage proteins are located in the endosperm and serve as a source of nitrogen and carbon during germination. Upon optimal growing conditions of light, temperature, and water, proteases in the seed cotyledon break down the storage proteins, providing the amino acids essential for protein synthesis and seed maturation (Preedy, Watson, & Patel, 2011). Humans exploit these storage proteins as a food source, and it is these proteins that are of particular interest for the understanding the hypolipidemic effect of soy.

#### 1.1.2.1 Glycinin

Glycinin is a globular protein that represents between 30-40% of total soy protein and is composed of six subunits. Each subunit is composed of typically one acidic (A) and one basic (B) polypeptide held together by a disulphide bridge in the following order: G1 ($A_{1a}B_{1b}$), G2 ($A_2B_{1a}$), G3 ($A_{1b}B_2$), G4 ($A_3B_4$), G5 ($A_5A_4B_3$), and a

newly identified G7 (Beilinson, Chen, Shoemaker, Fischer, Goldberg, & Nielson, 2002). Molecular weights for acidic subunits range between 36kDa and 42kDa, with A5 having a particularly low molecular weight of 12kDa; basic subunits have molecular weights of approximately 20kDa (Lakemond, de Jongh, Harmen, Hessing, Gruppen, & Voragen, 2000; Zarkadas, Gagnon, Poysa, Khanizadeh, Cober, et al., 2007). Subunits are visualized by gel electrophoresis in Figure 1.

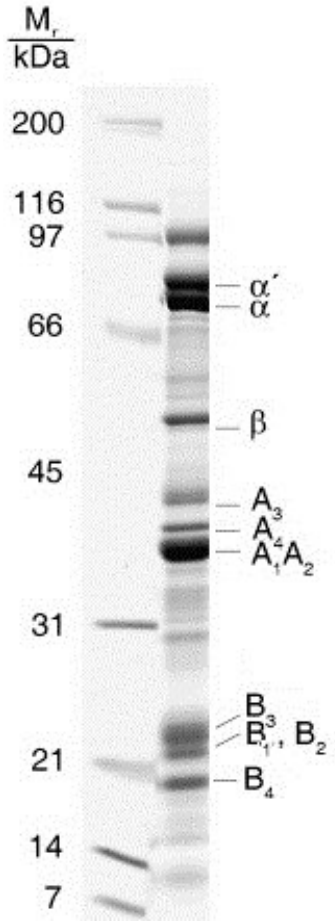


**Figure 1.1. Subunit composition of the wild-type soybean genotype (Harovinton).** Samples were run on an 8–18% gradient SDS-PAGE gel and were stained with Brilliant (Coomassie) Blue R250. A Precision Plus All Blue Prestained marker (Biorad; Cat. no. 1610373), and the molecular weights of the marker are noted. The principal storage polypeptide chains of glycinin and β-conglycinin are identified at the right of the gel. Image modified from Zarkadas et al. (2007). Permission granted from Elsevier.

In comparison, cysteine, glycine, methionine, and tryptophan are present in greater proportions in glycinin than in β-conglycinin. This accounts for the differences in protein interaction profiles between the two storage proteins. Glycinin has little to no interaction with carbohydrates but binds well with fibre molecules, which most likely accounts for the gel-forming ability of soy protein that is exploited in the production of tofu. Considering protein-lipid interactions, glycinin possesses more hydrophobic regions than β-conglycinin and high levels of lipids are found in glycinin isolates (Khatib, Herald, Aramouni, MacRitchie, & Schapaugh, 2002). This information is valuable for companies that rely on soy protein to increase foaming capabilities during food preparation (Wang, Troendle, Reitmeier, & Wang, 2012). Lipids impede foam formation; therefore, companies may be interested in glycinin null soybeans to increase product output. Interestingly, these protein-lipid interactions also appear to have functional significance with regards to cholesterol management. The 129-134 amino acid region of subunit A1a binds bile salt in the small intestine, thus inhibiting re-absorption, prompting increased bile excretion, and subsequently, reducing levels of cholesterol in the body (Choi, Adache, & Utsumi, 2002). Obesity-specific activity of glycinin is discussed in Section 1.3.

#### 1.1.2.2 β-conglycinin

β- conglycinin is the second-most abundant globular protein in soybean. It is composed of subunits α and α', whose N-terminals are homologous, and subunit β (Coates, Medeiros, Thanh, & Nielson, 1985). Molecular weights for these subunits

are 58kDa, 57kDa, and 42kDa, respectively (Petruccelli & Añón, 1995). Regarding composition, β-conglycinin contains a higher percentage of charged amino acids, such as arginine, aspartic acid, glutamic acid, and histidine, allowing for hydrophilic interactions and contributing to the emulsification and solubility properties of soy protein (Khatib et al., 2002).

Functionally, β-conglycinin does not interact with lipids to the same extent as glycinin, and it displays almost no interaction with fibre molecules; however, carbohydrate interactions are quite notable. Carbohydrate moieties, covalently bound to asparagine residues, contribute to up to 10% of total molecular weight (Khatib et al., 2002; Yamauchi, Thanh, Kawase, Shibasaki, 1975). It has been suggested that these moieties contribute to the allerginicity of this storage protein (Amigo-Benavent, Athansopoulos, Ferranti, Villamiel, & del Castillo, 2009).

Anti-obesity-specific activity of β-conglycinin is discussed in Section 1.3.

## 1.2 Adipose tissue

A healthy human body is composed of approximately 18% adipose tissue, although this percentage can vary significantly depending on gender and lifestyle (Marieb & Hoehn, 2007). Although homogenous in appearance, adipose tissue is composed of a variety of different cell types. Adipocytes, the lipid-storage cells, comprise only 50% of human adipose tissue; animal adipose tissue only contains 30% adipocytes (Cornelius, MacDougald, & Lane, 1994). The rest of the tissue is

composed of blood vessels, macrophages, and a collagen-rich extracellullar matrix (Ali, Hochefeld, Myburgh, & Pepper, 2013; Khan, Muise, Iyengar, Wang, Chandalia, Abate et al., 2009).

There are two types of adipose tissue: white (WAT) and brown (BAT). Functionally, WAT serves as a storage site for excess triglycerides, a cushioning layer for body organs, and an insulating layer to maintain body temperature (Ali et al., 2013). By contrast, brown adipose tissue is highly vascularised and serves as a thermogenic organ in the body (Moreno-Navarrete & Fernández-Real, 2012). WAT and BAT are further explained in Sections 1.2.1 and 1.2.2, respectively.

### 1.2.1 White adipose tissue (WAT)

WAT depots are classified based on their location within the body. Adipose tissue is often stored under the dermis, termed "subcutaneous" fat, but it may also be found around the internal organs and in the omentum of the abdominal cavity, termed "visceral" fat. Women typically store excess adipose tissue subcutaneously in the gluteal-femoral region, leading to a pear-shaped physique. Men tend to store excess adipose tissue in the abdominal cavity, leading to an apple-shaped physique (White & Tchoukalova, 2013). Visceral fat poses a greater risk for metabolic disease than subcutaneous fat. Visceral adipose tissue contains fewer pre-adipocytes, the precursors to mature lipid-storing adipocytes, and thus resorts to cellular hypertrophy instead of increasing cell populations to accommodate lipid storage (Further explanation of adipocyte development is found in Section 1.2.3). Enlarged adipocytes are less responsive to insulin, leading to decreased lipid storage in

adipose tissue and increased ectopic lipid storage (Yang, Eliasson, Smith, Cushman, & Sherman, 2012).

The main cellular body of white adipocytes is dominated by a large lipid droplet which forces the cytoplasm and the nucleus to the outer edge of the cell (Moreno-Navarrete & Fernández-Real, 2012). Excess dietary lipids sequestered in lipoprotein particles called chylomicrons and free glucose are ferried in the blood and delivered to adipocytes where glucose enters through the GLUT4 channel and freed fatty acids enter with the assistance of lipoprotein lipase (LPL). Glucose passes through the glycolytic pathway to form pyruvate, which is eventually converted to fatty acyl- CoA through a series of steps, and glycerol 6-phospate, as a by-product. Glycerol 6-phosphate and fatty acyl-CoA, derived from both glucose and chylomicron delivery, undergo esterification to form triglyceride, the primary form of lipid storage. Esterification is mediated by membrane-bound LPL; low LPL levels correspond with low free fatty acid uptake by adipocytes (Zechner, Strauss, Frank, Wagner, Hofmann, Kratky, et al., 2000).

As a consequence of its role as the primary lipid storage tissue, WAT responds to hormonal and nervous signals in order to regulate total energy availability in the body (refer to Figure 1.2). In WAT, stored triglycerides may be mobilized by glucagon signalling. Generally, white adipocyte functioning is dependent on cell size; as previously mentioned, larger cells, which are typically found in obesity, are less efficient at responding to external hormonal stimulation and storing triglycerides (Kanda, et al., 2006). Consequently, excess dietary lipids

begin accumulating in other tissues, such as bone, muscle, and organs. This ectopic fat deposition has been identified as a potential cause of several chronic illnesses such as high blood glucose, hypertension, atherosclerosis, Type II diabetes, and osteoporosis (Ali et al., 2013; Gregoire, 2001; Xu, et al., 2003).

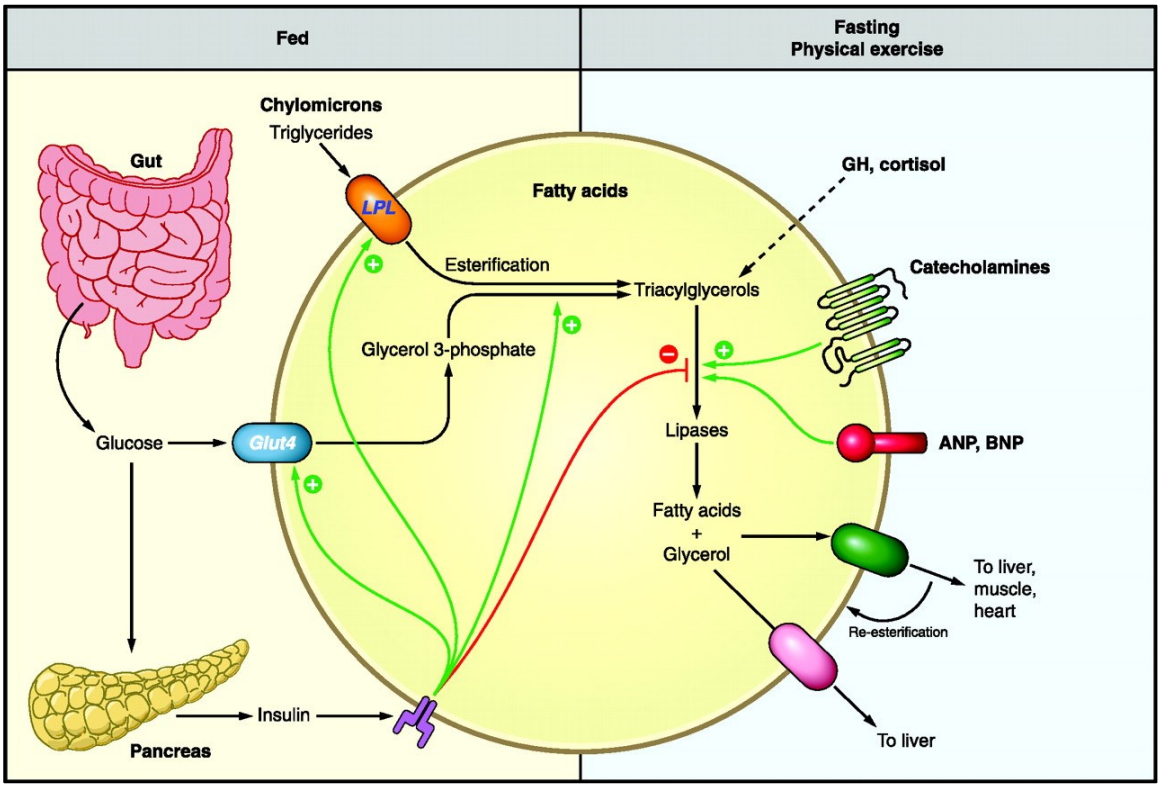


**Figure 1.2.** Hormonal and nervous control of lipid storage and mobilization in an adipocyte. GH refers to growth hormone, ANP refers to atrial natriuretic peptide, BNP refers to brain natriuretic peptide, and LPL refers to lipoprotein lipase. Taken from Thompson, Karpe, Lafontan, & Frayn (2012). No formal permission required by Physiological Reviews for thesis publication.

WAT also exhibits endocrine functions which impact glucose metabolism, appetite, blood pressure, and immunity. Adipocytes release leptin, adipsin, and adiponectin, angiotensinogen and resistin, polypeptides whose responsibilities include regulation of satiety, immune response, increased fat and glucose breakdown, vasoconstriction, and increased blood lipoprotein levels, respectively (Ali et al., 2013). Thus, WAT is a much more dynamic tissue than simply a storage site for lipids in the body.

Obesity often results in large-diameter adipocytes due to the imbalance between caloric storage demands and adipose tissue hyperplasia (Lessard & Tchernof, 2012). Enlarged adipocytes hinder healthy adipose tissue functioning. Cell size increases, adipocytes produce more pro-inflammatory signals which have systemic impact. Pro-inflammatory signals include tumour necrosis factor alpha (TNF-α), interleukin-6 (IL-6), interleukin-8 (IL-8), interleukin-10 (IL-10), and monocyte chemoattractant protein-1 (IL-1) (Kanda et al., 2006; Tordjman, Guerre-Millo, & Clément, 2008). Moreover, adipokines attract large macrophage populations to take up residence within adipose tissue, leading to increased pro-inflammatory signalling and subsequent impaired body metabolism. Additionally, TNF-α interacts with GLUT4 receptors in skeletal muscle, rendering them insensitive to insulin signalling and decreasing glucose absorption (Coppack, 2001). Insulin insensitivity in myeloid, hepatic, and adipose tissue is further aggravated IL-1, IL-8, and TNF-α through the activation Jun N-terminal kinase and inhibitor of κβ kinase; these kinases phosphorylate various proteins in the insulin-signalling cascade, thereby rendering them non-functional (Arkan, Hevener, Gretan, Maeda, Li,

Long, et al., 2005; Hirosumi, Tuncman, Chang, Görgün, Uysal, Maeda, et al., 2002). Adipokines have also been associated with increased hepatic lipogenesis and elevated serum triglyceride levels (Feingold & Grunfeld, 1987). WAT development and lipid accumulation are the primary focuses of this study.

### 1.2.2 Brown adipose fat (BAT)

Morphologically, BAT differs from WAT. Brown adipocytes have many lipid droplets and a large population of mitochondria, thus making BAT a more metabolically active tissue (Moreno-Navarrete & Fernández-Real, 2012). BAT also is much more vascularised and innervated than WAT. Nocturnal and hibernating mammals have the largest stores of BAT; human newborns have small patches of this tissue around the body, but BAT deposits decrease significantly over time (Canon & Nedergaard, 2004).

As previously mentioned, BAT is a thermogenic tissue due to the expression of uncoupling protein -1 (UCP-1). In the electron transport chain, UCP-1 serves as a proton channel, ferrying $H^+$ ions down their concentration gradient (Seale & Lazar, 2009). Unlike ATP synthase in the electron transport chain that uses the energy of $H^+$ ions travelling down their concentration gradient to create ATP, UCP-1 does not use the released energy. Instead, the energy produced by the moving $H^+$ ions is released as heat (Canon & Nedergaard, 2004). This seemingly inefficient system permits maintenance of core body temperature for animals in cold weather and for newborns to combat cold shock upon birth (Seale & Lazar, 2009).

Due to its high metabolic activity, there has been growing interest in BAT and its potential role in the treatment of obesity. Rat studies have shown an increase in BAT as a result of increased caloric intake, a phenomenon termed "diet-induced thermogenesis" (Rothwell & Stock, 1983). A recent bovine study identified a novel form of preadipocytes that are able to differentiate into brown adipocytes upon dietary stimulation (Asano, Yamada, Hashimoto, Umemoto, Sato, Ohwatari, et al., 2013). Further studies are required to determine whether these observations can be extrapolated to humans. Still, BAT does appear to play some role in human weight management. Asano et al. (2013) recorded that brown adipocytes are still present in adult humans, although the population is small and often interspersed within WAT. Moreover, studies showed that lean people have lower levels of WAT and higher levels of BAT than their obese counterparts, thus confirming that BAT may indeed be a powerful tool for combatting obesity (Cypress, Lehman, Williams, Rodman, Goldfine, Kuo, et al., 2009). Despite the potential anti-obesity effects of BAT, this project focuses primarily on the effect of soy on WAT.

### 1.2.3 Adipogenesis

As previously mentioned, adipocytes are the lipid-storing cells in adipose tissue. Ten percent of the body adipocyte population is regenerated every year; however, mature cells are terminally differentiated, meaning they are unable to undergo mitosis. Adipocyte population growth is thus dependent on the mitotic division of preadipocytes (Ali et al., 2013). Preadipocytes are immature adipocytes that are unable to store triglycerides. While their lineage is still unclear, it has been

speculated that preadipocytes derive from multipotent mesenchymal cells through a combination of chemical triggers such as insulin and poly-unsaturated fatty acid-induced cAMP signalling *in vivo* (Fujikura, Fujimoto, Yasue, Noguchi, Masuzak, et al., 2005; Madsen, Pederson, Liaset, Ma, Petersen, et al., 2008). *In vitro*, the following chemical triggers are used to prompt differentiation: fetal bovine serum (FBS), insulin, dexamethasone, and 1-methyl-3-isobutylxanthine (Götherström, Ringdén, Westgren, Tammik, & Le Blanc, 2002). Upon detection of the aforementioned chemical signals, other mammalian mesenchymal cells undergo mitosis to form a clonal population of committed cells; human adipocytes do not require this step (Gregoire, 2001). Cells then enter first growth arrest to halt cell expansion and prepare for division. Mitotic clonal expansion occurs to increase the preadipocyte population. The increasing population of preadipocytes serves as a negative inhibition signal for mesenchymal cell commitment; contact inhibition between neighbouring preadipocytes prompts cells to enter second growth arrest (Rosen & Spiegelman, 2000). Once again, chemical triggers, such as insulin, cAMP, and *in vitro*, dexamethasone, signal for differentiation to occur. Proteolytic enzymes are released by preadipocytes to degrade the surrounding extracellular matrix to allow for a morphological change from elongated fibroblastic shape to ovoid (Gregoire, 2001). Cells fill with triglycerides and pack tightly together to form WAT. Angiogenesis also occurs in tandem with adipogenesis to provide the required vascularization for newly developing tissue (Ali et al., 2013). As humans age, adipogenesis-related genes are less active, resulting in an overall decrease in the

rate of adipogenesis and an inefficiency in triglyceride storage in adipocytes (Kirkland, Hollenberg, & Gillon, 1993).

#### 1.2.3.1 Peroxisome proliferator-activated receptor γ (PPARγ)

The transformation of preadipocytes into mature adipocytes is controlled by a series of genetic regulators, including transcriptional factor sterol-regulatory-element-binding-protein-1 (SREBP1), single transducers and activators of transcription (STATs), enhancer binding protein α, β and δ, peroxisome proliferator-activated receptor γ (PPAR γ), and CCAAT/ enhancer-binding protein (C/EBP -α, -β, -δ) (Ali et al., 2013).

Peroxisome proliferator-activated receptor γ is the regulator of interest in this report. PPARs are a group of ligand-dependant transcription factors from the nuclear hormone receptor superfamily that heterodimerize with retinoid X receptors and bind the DNA at specialized regions called peroxisome proliferator response elements (PPREs) to initiate transcription of downstream genes (Larson, Toubro, & Astrup, 2003). Different subtypes (α, δ, λ) are predominantly found in various tissues in the body, and each serves a slightly different function. PPARα is highly expressed in muscle, heart, kidney, and liver tissue and up-regulates the expression of enzymes involved in fatty acid oxidation (Leff, Matthews, Camp, 2004). The transcription factor is also involved in up-regulating peroxisome expression in hepatic tissue, thus giving the group its name (Larson et al., 2003). PPARδ, although expressed in almost all tissues, is functionally more obscure; studies have linked the transcription factor to downstream protein involved in

wound healing and cholesterol transport, among other processes (Leff et al., 2004; Michalik, Desvergne, Tan, Basu-Modak, Escher, Rieusset et al., 2001). Conversely, PPARγ is much better understood and will be considered in more detail as it is the regulator of interest in this report.

PPARγ exists in two isoforms in humans and rodents, isoform one and two (PPARγ1 and PPARγ2, respectively). PPARγ1 is found in adipose tissue, skeletal muscle, bone, pancreatic tissue, and liver tissue whereas PPARγ2 is more abundant in white and brown adipose tissue. PPARγ2 possesses 28 additional amino acids at the N-terminal, which enables this isoform to be more ligand-independent than PPARγ1 (Deeb, Fajas, Nemoto, Pihlajamaki, Mykkanenen, et al., 1998). Interestingly, PPARγ2 expression is influenced by nutrition; high fat diets cause ectopic expression of the transcription factor and subsequent unwanted lipid accumulation in skeletal muscle and liver tissue (Medina-Gomez, Gray, & Vidal-Piug, 2007). As a result, PPARγ2 is the noteworthy isoform in obesity studies.

In adipogenesis, second growth arrest is mediated by PPARγ (Rosen & Spiegelman, 2000). Siersbaek, Nielsen, & Mandrup (2012) described the transcriptional networks involved in adipogenesis. Chemical signals, as described in Section 1.2.3, activate a series of transcription factors, termed early adipogenic factors, which in turn lead to the up-regulated expression of PPARγ (Figure 1.3).

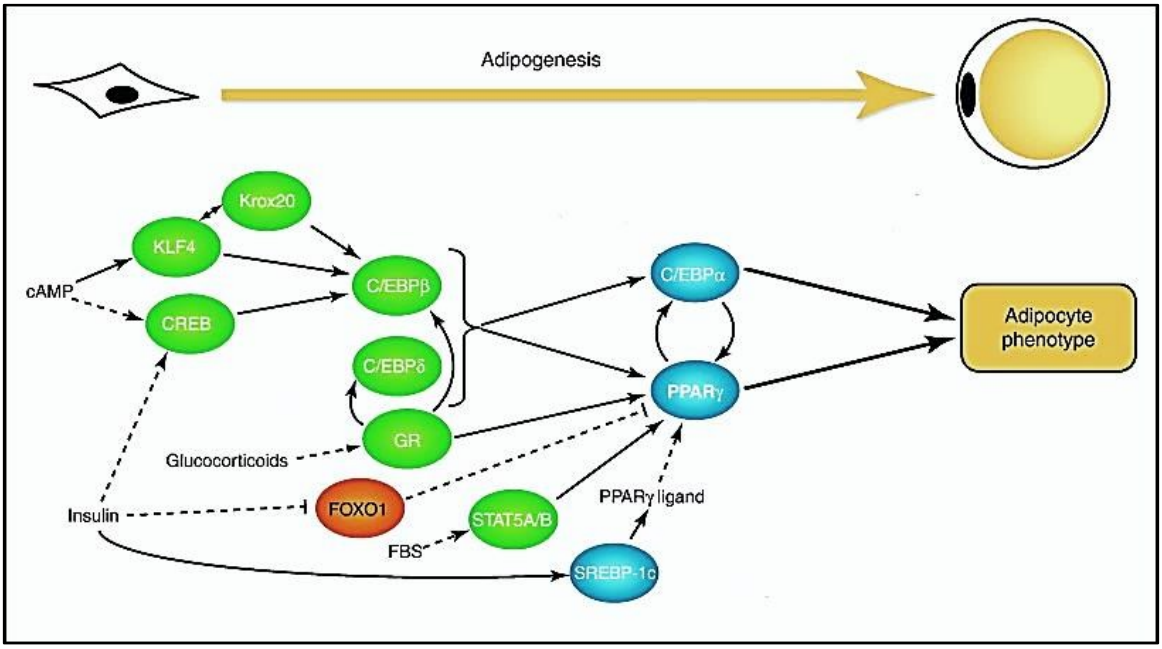


**Figure 1.3. Activation of PPARγ and adipogenesis.** Early adipogenic factors are identified in green, anti-adipogenic factors are shown in orange, and late adipogenic factors are shown in blue. Solid arrows represent up-regulation of gene expression. Dashed arrows represent up-regulation of activity. Dashed lines with flat ends represent inhibition of activity. Abbreviations: CCAAT/enhancer-binding protein α, β and δ (C/EBP –α, -β and –δ); cyclic AMP (cAMP), cAMP response element binding protein (CREB), forkhead box 01 (FOX01), glucocorticoid receptor (GR), Krüpel-like factor (KLF4), early growth response 2 (Krox20), sterol regulatory element-binding protein 1c (SREBP-1c), and signal transducer and activator of transcription 5A/B (STAT5A/B). Image modified from Siersbaek et al. (2012). Permission granted from Elsevier.

PPARγ heterodimerizes with a second transcription factor, retinoid X receptor, and binds to the PPRE in the downstream genes to re-program the cell for the development of a mature, lipid-accumulating physiology (Leff et al., 2004). Examples of genes up-regulated by PPARγ include *c/ebpα, e2f/dp, gata2, gata3, and wnt-1*; with the exception of *wnt-1*, the expressed proteins are transcription factors that have downstream effects on required protein expression for adipogenesis (Ali, et al., 2013; Goto, Mori, & Nagaoka 2013; Rosen & Spiegelman, 2000). Wingless-type MMTV integration site *(*wnt-1) protein is the first step in a signalling network designed to coordinate the body's energy availability and pre-adipocyte differentiation and lipid accumulation (Christodoulides, Lagathu, Sethi, & Vidal-Puig, 2009). Further downstream, PPARγ has been shown to up-regulate the expression of proteins involved in lipid accumulation in mature adipocytes, including the trans-membrane lipid transporter fatty acid-binding protein 4 (FABP4), and the adipocytokines adiponectin, and adipsin (Nakachi, Yagi, Nikaido, Bono, Tonouchi et. al., 2008).

PPARγ and C/EBPα appears to bind in similar chromatin regions, lending to cooperative activity. C/EBPα also serves as a positive feedback signal for PPARγ activity (Rosen & Spiegelman, 2000). In this way, differentiation runs to completion, converting preadipocytes into mature adipocytes. While PPARγ and C/EBPα work together to promote differentiation, studies have shown that PPARγ may be the more important regulator of this process. Addition of PPARγ to C/EBP$^{-/-}$α murine embryos restored adipocyte differentiation, but addition of C/EBPα to *PPARγ*$^{-/-}$ murine embryos did not restore adipocyte differentiation (Rosen, Hsu, Wang, Sakai,

Freeman, Gonzalez, et al., 2002; Wu, Rosen, Brun, Hauser, Adelment, Troy et al., 1999).

As previously mentioned, PPARγ is ligand-dependent. PPARγ ligands are lipid derivatives, usually poly-unsaturated fatty acids, and may be either endogenous or dietary. Examples of endogenous ligands include 9- and 13-hydroyxyoctadecadienoic acid particles derived from lipoproteins, and 15-deoxy-*[DELTA]*- prostaglandin J2, a metabolite of arachidonic acid (Devergne & Wahli, 1999). ADD1 and SREBP1, two transcription factors, have been shown to work cooperatively to promote the production of an endogenous PPARγ ligand (Rosen & Speigelman, 2000). Eicosapentanoic acid is an example of a diet-derived ligand (Devergne & Wahli, 1999).

### 1.3 Recent research

Current research has primarily focused on the effect of soy isoflavones in lipid metabolism. Rodent studies revealed that soy isoflavone and protein mixtures resulted in reduced plasma HDL levels and increased fecal excretion of neutral sterols and bile acid (Lin, Meijer, Vermeer, & Trautwein, 2004). Xiao, Wood, Weber, Aziz, Mehta, et al. (2013) fed a low-fat diet supplemented with soy protein isolate (SPI) and soy isoflavone concentrate to Sprague-Dawley rats. The study revealed an up-regulation of hepatic lipolytic and β-oxidative genes and a down-regulation of hepatic lipogenic genes, such as PPARγ and fat-specific protein 27, leading to elevated serum free fatty acid levels. Specific focus on the response of adipose tissue to soy isoflavones revealed conflicting results. No overall weight loss was

observed; dorsal adipose depots within the body decreased, due to up-regulated lipolytic genes and down-regulated lipogenic genes, but abdominal and retroperitoneal adipose depots increased in mass (Jiang, Li, Fan, Zhang, Osa, et. al., 2015).

Speculation as to the bioactivity of soy protein independent of isoflavones led to further investigation. These studies revealed that soy protein may indeed have an impact on lipid metabolism. Rats fed diets supplemented with β-conglycinin demonstrated preferential consumption of carbohydrates versus lipids. Moreover, β-conglycinin consumption prompted reduced serum triglyceride levels, complementing the results observed by Xiao et al. (2013) (Inoue, Fujiwara, Kato, Funayama, Ogawa, et al., 2015).

Since PPARγ is the key regulator of the second growth stage of adipogenesis, studies have also focused on the effect of soy protein on PPARɣ. Yamazaki, Kishimoto, Muira, & Ezaki (2012) considered the response of hepatic PPARɣ in the presence of dietary β-conglycinin. The *in-vivo* murine study determined that an unknown sub-peptide of the main β-conglycinin molecule may be involved in down-regulating PPARɣ2 expression in hepatocytes, thereby decreasing lipid accumulation in the liver. This effect was not observed in WAT. Later *in-vivo* murine liver studies revealed interactions between soy protein and the WNT/β-catenin pathway (WNT was briefly discussed in Section 1.2.3.1). WNT is responsible for inhibiting PPARγ-mediated adipogenesis and lipid accumulation in the liver, skeletal muscle, and adipose tissue. Soy protein was shown to down-regulate the

expression of WNT antagonists normally seen in obesity, thereby allowing WNT to effectively inhibit PPARγ and prevent hepatic lipid accumulation (Zhou, Lezmi, Wang, Davis, Benz, et al., 2014).

The present study aims to build on previous research in order to more thoroughly understand the interaction between adipose tissue PPARγ and specific soy proteins. Goto, Mori, & Nagaoka (2013) re-evaluated the impact of soy peptides on PPARγ in adipose tissue using *in vitro* experimentation. Contrary to the study performed by Yamazaki et al. (2013), they observed that soy peptides up-regulated PPARγ expression and increased adipocyte differentiation. This difference may be attributed to tissue-specific effects of soy protein on PPARγ. Additionally, the study showed increased insulin sensitivity in adipocytes, which may be beneficial for preventing obesity-induced diabetes. When considering the effect of specific soy proteins on lipid metabolism, specific focus was given to glycinin and β-conglycinin. *In vivo* experiments revealed a decrease in abdominal adipose tissue and serum free fatty acids with soy-supplemented diets. This was a notable physiological response since soy isoflavone experiments had shown conflicting results regarding abdominal tissue development (Jiang, Li, Fan, Zhang, Osa, et. al., 2015). Further analysis of the soy peptides revealed that the α' subunit of β-conglycinin and the A1-5 glycinin subunits were not involved in the observed results (Chen, Wood, Gagnon, Cober, Frégeau-Reid, et al., 2014; Yamazaki et al., 2012). Therefore, a bioactive soy peptide involved in adipose tissue development remains to be identified.

## 1.4 Objectives and Hypotheses

The overall aim of the study was to identify the bioactive soy protein subunit that may be responsible for the observed reduction of abdominal adipose tissue in rats.

The first objective of this project was to observe the effect of soy protein on adipocyte differentiation and lipid accumulation. Specifically, the Harovinton and 1a knock-out soy strains were considered. Harovinton strain is a common Canadian tofu type cultivar, and 1a is a knock-out line developed by Agriculture and Agri-Food Canada. Both strains were genetically characterized and very similar in fibre, ash, and fat composition, thus allowing for confident analysis of the effect of the individual soy storage proteins. Adipose tissue morphology was observed to identify any notable differences in differentiation or lipid accumulation in response to soy protein.

The second objective was to consider a relationship between soy peptides and PPARγ expression in adipose tissue, both *in vitro* and *in vivo*. Based on the literature, it was predicted that PPARγ expression will increase in the presence of soy peptide.

Much of the study was performed both *in vivo* and *in vitro* in order to gain a complete picture of the effect of soy protein on gene expression and physiology of adipose tissue.

# 2 CHAPTER: MATERIALS AND METHODS

## 2.1 Soy strain information

The Harovinton soy strain was developed by the Agriculture Canada Research Station, Harrow, Ontario (Buzzell, Anderson, Hamill, & Welacky, 1991). The SQ97-0263_3-1a (henceforth referred to as "1a") soybean strain was developed by Dr. V. Poysa at the Greenhouse and Processing Crops Research Centre, Harrow, ON (Zarkadas, Gagnon, Poysa, Khanizadeh, Cober, et al., 2006). The 1a strain, a cross product of the Harovinton cultivar and the Iwate-3 cultivar provided by Dr. N. Kaizuma, Iwate University, Morioka, Iwate, Japan, was a null strain for the following storage protein subunits: β-congycinin α', and glycinin A1a, A1b, A2, A3, and A4 (note that the corresponding basic subunits were also knocked out. Refer to 1.1.2.1 for a complete list of genes and associated subunits). Harvinton and 1a soybeans were grown from AAFC breeder seed tofu in the same season and field. Tofu was prepared according to the protocol outlined in Chen et al. (2014). To summarize, soybeans were ground and pressure-cooked to extract the soy milk. Glucono-delta-lactone (Sigma-Aldrich, St-Louis, MO, USA; Cat. no. G4750) was added to the slurry at to a final concentration of 0.3% (w/v) for coagulation. The curds were extracted and freeze-dried for storage until further use.

Casein was obtained from Harlan Teklad, Madison, WI, USA. Soy protein isolate devoid of isoflavones (SPI) (PRO-FAM®-930), and Novasoy isoflavone (ISF) concentrate were obtained from Archer Daniels Midland Company (Decatur, IL, USA).

### 2.1.1 Soy protein preparation

Casein and soy protein hydrosylates were prepared for future cell culture experiments. For each soy strain, approximately 25g of freeze-dried tofu sample were de-fatted using the Dionex ASE200 Accelerated Solvent Extraction System (Thermo Scientific, Waltham, MA, USA) and three cycles of the following protocol at 4000psi: heating for five minutes at 55°C, temperature stabilization at 55°C for ten minutes, and wash in petroleum ether for 60 seconds. The de-fatted samples were ground into a fine powder using a mortar and pestle and stored at $4^0$C until further use.

For isoflavone elimination, de-fatted samples were washed at a ratio of five grams of tofu to 100mL of 80% methanol for one hour at 60-65°C with constant stirring. Upon filtration, the mixture was filtered using vacuum filtration. The soy samples were washed another two times in methanol and stored at 4°C for further use. The isoflavone elimination was performed for all 25g of de-fatted soy.

Protein hydrolysis was performed in five gram batches. Five grams of soy were added to 100mL of distilled water and heated to 85°C in a water bath. The mixtures were then cooled to 37°C, and the pH was adjusted to 2.0 using 12M HCl. Protein digestion was performed through the incubation of the mixtures with 300mg of pepsin (Sigma, Cat. no. P700) for 30 minutes with constant stirring. $Na_2CO_3$ powder was used to adjust the pH to 7.0, and the mixture was incubated with 300mg of pancreatin (Sigma, Cat. no. P1750 x 4 USP) for one hour at 37°C with constant stirring. Enzymatic digestion was halted by heating the mixture to 85°C for

15 minutes. The digested protein samples were manually freeze-dried using liquid nitrogen and methanol and stored in dry ice for one week for complete drying. The samples were then stored at -20°C for long-term storage.

## 2.2 Animal study

The animal study was performed according to the methods described in Chen et al., 2014. Briefly, eight week-old male and female Sprague-Dawley rats (Charles River, QC, Canada) were individually housed on a 12 hour dark/light cycle with free access to water and diets prepared in accordance with the American Institute of Nutrition Rodent Diet -93G (AIN-93G) for 12 days. Following acclimation, rats were randomly divided into five groups and fed diets containing 20% protein deriving from casein, SPI, or freeze-dried tofu from the developed soy lines (Table 1). With the exception of SPI, all soy- supplemented diets contained isoflavones (tofu samples did not undergo methanol elimination of isoflavones). Descriptions of diets with corresponding protein sources are found in Table 1. Following eight weeks of being fed experiemental diets, rats were euthanized, and adipose tissue was harvested and stored at -80°C for further use. The animal study adhered to the guidelines set by the Canadian Council for Animal Care and was approved by the Health Canada Animal Care Committee.

**Table 1**. Protein and isoflavone supplementation in the diets fed to Sprague-Dawley rats (g/kg diet). Rats were fed the AIN-93G rodent diet, which contained 339.12g to 357.61g of corn starch, 82g of dextrinized corn starch, 51g of lard, and 93g to 100g of sucrose. Data obtained from Chen et al. (2014).

| Diet | Protein in diet | L- methionine supplementation | L- cysteine supplementation | Isoflavone addition[a] | Total Isoflavone |
|---|---|---|---|---|---|
| Casein[b] | 200 | 3.00 | | | |
| Casein[b] and ISF | 200 | 3.00 | | 0.17 | 0.05 |
| SPI[b] | 200 | | 3.00 | | 0.05 |
| Harovinton | 200 | | 3.00 | | 0.70 |
| 1a[c] | 200 | | 3.00 | | 0.70 |

[a] Novasoy Isoflavones used for isoflavone supplementation.
[b] Supplement contained 90% crude protein.
[c] 1a refers to the knocked-out strain SQ97-0263_3-1a with the following null profile: β conglycin a', glycinin A1a A1b A2 A3 A4.

## 2.3 Cell culture information

Mouse preadipocytes (3T3-L1) (ATCC, Manassas, VA, USA; Cat. no. CL-173™) were seeded at a density of 2.0 x $10^4$ cell/mL on either 24-well plates with 1mL of growth media or 100mm x 20mm dishes with 10mL of growth media (these are the standard media volumes for all future media changes). Growth media composition was as follows: 90% Dulbecco's Modified Eagle's Medium (DMEM) (ATCC; Cat. no. 30-2002), 10% iron-fortified bovine calf serum (ATCC; Cat. no. 30-2030), 0.1% penicillin-streptomycin or penicillin-streptomycin/Fungizone® (Gibco/Life Technologies, Burlington, ON, CA; Cat. no. 15140 and 15240). Cells were grown for seven days at 37°C and 5% $CO_2$ with the media being changed every 48hrs.

### 2.3.1 Treatment optimization

For certain experiments, rosiglitazone (Cayman Chemicals, Ann Arbor, MI, USA; Cat. no. 71740) served as a positive control. Rosiglitazone concentration optimization was determined through the administration of a concentration gradient (a final concentration of 1µM to 8µM rosiglitazone dissolved in DMSO per well) with the differentiation media on day 7. Visual observations using the EVOS fl microscope on day 12 were used to determine the optimal concentration. The optimal concentration was defined as the amount of rosiglitazone that prompted the most differentiation and lipid accumulation in the 3T3-L1 cells with a minimal amount of cell sloughing. The chosen concentration was used as the dosage concentration for subsequent experiments.

Casein and soy treatment optimizations were performed in a similar fashion with minor modifications. Casein and Harovinton were dissolved in water and administered in a concentration gradient of 25µg/mL to 400µg/mL. The optimal concentration was defined as the amount of casein that prompted the most differentiation and lipid accumulation in the 3T3-L1 cells with a minimal amount of cell sloughing. The Harovinton concentration gradient was used to confirm the optimal concentration determined by casein. Visual observations using the EVOS fl microscope were used to determine the optimal concentration, which was used as the dosage concentration for subsequent experiments.

### 2.3.2 Differentiation

On day 7, cells were incubated in differentiation media (90% DMEM, 10% fetal bovine serum (FBS) (Gibco; Cat. no. 12484), 1.0µM dexamethasone (Sigma; Cat. no. D8893), 0.5mM 3-isobutyl-1-methylxanthine (IBMX) (Sigma; Cat. No. 17018), 0.1% penicillin-streptomycin/Fungizone®, and 1µg/mL bovine insulin (Gemini Bio-Products/Cederlane, Burlington, ON, CA; Cat. no. 700-912P)) for 48 hours. After 48 hours, cells were provided with fresh post-differentiation media (90% DMEM, 10% FBS, 1.0µg/mL insulin) and grown for another five days with media change every 48 hours.

Protein treatments were administered either on day 7 with the differentiation media or on day 9 with post-differentiation media. For treatment time points, casein or soy protein hydrolysates were dissolved in dd$H_2O$, sterilized by filtration, and administered at a final concentration of 200µg/mL. Rosiglitazone was

administered at a final concentration of 6μM. For information on the protein, refer to Section 2.1.2.

## 2.4 Lipid droplet measurement assay

### 2.4.1 Cell culture

The cells were grown in 24-well plates according to the protocol outlined in Section 2.3. Protein and rosiglitazone treatments were administered at both time points described in Section 2.3.2.

### 2.4.2 Cell staining

The cells were fixed in 10% formalin for one hour at room temperature. The cells were then rinsed three times with water and were incubated with 500μL of 60% isopropanol for five minutes at room temperature. The washed cells were stained with 500μL of 2mg/mL Oil Red O solution (Amresco, Solon, OH, USA; Cat. no. 0684-250) for ten minutes at room temperature. Excess dye was washed away with three rinses of water. The cells were incubated with 500μL of hematoxylin (Sigma; Cat. no. HHS16-500) for one minute, and excess dye was removed with three rinses of water. The cells were kept moist with the addition of 250μL of $dH_2O$ to each well.

### 2.4.3 Statistical analysis

Images of the cells were acquired using the EVOS® XL bright field microscope (Life Technologies; Cat. no. AMEX3300). Lipid droplet measurements were obtained using phase contrast microscopy and the Northern Eclipse 1.0 software.

Three images were taken for each treatment, and all droplets in the field of view were measured. Data from the three images were combined to obtain the total number of lipid droplets. Percent distributions for the different size categories were determined for each by dividing the number of droplets within a size category by the total number of lipid droplets. Percent distributions were averaged for the six replicates to obtain the final results. Statistical significance was defined as $p<0.05$ and was determined by one-way ANOVA and Fisher LSD analysis using SigmaPlot 12.5.

## 2.5 Oil Red O quantification assay

### 2.5.1 Hoescht standard curve

Mouse preadipocytes (3T3-L1) were seeded at densities ranging from $5 \times 10^3$ to $8 \times 10^4$ on 24-well plates (Corning, Corning, NY, USA; Cat. no. 3527) with 1mL of growth media and grown for 24 hours. The cells were washed in 1x PBS and fixed in 500mL of 10% formalin solution (10% formaldehyde (Sigma; Cat. no. F8775), 3.3mM $NaH_2PO_4$, 4.6mM $Na_2HPO_4$) for one hour at room temperature. The cells were rinsed three times with water and incubated with 500µL of 2µM Hoescht solution. The cells were rinsed three times with water and then fluorescence was detected using the Tecan Infinite M200PRO and Tecan iControl 1.7 software (San Jose, CA, USA) (excitation 343nm, emission 483nm).

### 2.5.2 Cell culture

The cells were grown in 24-well plates according to the protocol outlined in Section 2.3. Protein and rosiglitazone treatments were administered at the time of differentiation (day 7) described in Section 2.3.

### 2.5.3 Cell staining

The cells were incubated with 500µL of 10% formalin for one hour at room temperature and stained with Hoescht on day 12 following the procedure found in Section 2.5.1. After the fluorescent detection, the cells were incubated with 500µL of 60% isopropanol for five minutes at room temperature. The cells were then stained with 500µL of 2mg/mL Oil Red O solution as described in Section 2.4.2. The cells rested for a minimum of one hour in dd$H_2O$, and then the dye was extracted. The wells were washed twice with 60% isopropanol for five minutes and then once with 250µL of 100% isopropanol for five minutes. Two hundred microliters of the final wash was transferred to a 96-well plate and the absorbance was read at 492nm.

### 2.5.4 Statistical analysis

Background interference was subtracted from absorbance readings, and the new values were divided by the Hoescht absorbance readings. Fold differences were determined by dividing the normalized absorbance readings by the No Treatment normalized absorbance. Average fold differences were determined using

the 14 experimental replicates. Statistical significance was defined as $p<0.05$ and was determined by one-way ANOVA and Fisher LSD analysis using SigmaPlot 12.5.

## 2.6 qPCR analysis

### 2.6.1 RNA extraction from adipose tissue and cDNA synthesis for qPCR analysis

Total RNA extraction was performed using the RNEasy Mini Kit (Qiagen, Toronto, ON, Canada; Cat. no. 74104) with the manufacturer's instructions with the following modifications. Approximately 200mg of adipose tissue from male rats was ground into powder in sterile 1.5mL microfuge tubes using small plastic pestles. Cell lysis was performed by vortexing the samples for one minute in 1mL of QIAzol (Qiagen; Cat. no. 79306). The mixture was then stored overnight at -20°C, and a thick lipid layer was removed the following morning. Samples were then treated for further lipid removal through the addition of 500µL 100% chloroform. The mixtures were vigorously shaken for 15 seconds then left to sit at room temperature (23°C) for 10 minutes. The tissue homogenates were centrifuged for 15 minutes at max speed and 4°C. The upper aqueous layer of each sample was transferred into second sterile 1.5mL tube, to which 700µL of 70% ethanol was added to each sample. The mixtures were chilled at -20°C for 20 minutes and loaded on the mini prep column. A DNase digestion was also performed according to the manufacturer's instructions using the RNase-Free DNase Set (Qiagen; Cat. no. 79254). Following the final set of washes, RNA was eluted using 30µL sterile water.

Concentrations were analyzed using the NanoDrop 1000 (Thermo Scientific). All RNA extractions were performed on the same day to limit variability.

RNA extracts were converted to cDNA using the RT$^2$ First Strand Kit (Qiagen; Cat. no. 330401) according to the manufacturer's instructions.

### 2.6.2 Adipogenesis array

RT$^2$ Rat Adipogenesis array plates (Qiagen; Cat. no. PARN-049Z) were used for broad spectrum expression analysis on male rat adipose tissue samples. Mastermixes were prepared fresh using 102µL of cDNA, 1350µL of RT$^2$ SYBR Green qPCR Mastermix (Qiagen; Cat. no. 330512), and 1248µL of RNase-free water, according to the manufacturer's instructions. Twenty microliters of the mix was distributed into each well, and the qPCR was performed on the Biorad CFX96 Touch Real-Time PCR Detection System (Hercules, CA, USA; Cat. no. 185-5196) using the following protocol: hot start activation at 95$^o$C for 10 minutes, followed by 40 cycles of 15 seconds at 95$^o$C and 1 minute at 60$^o$C. Eight biological repetitions were used for this assay.

### 2.6.3 Statistical analysis

Data was analyzed using the gene study function in the BioRad CFX Manager 3.1 software. Normalized expression was determined using the housekeeping genes present on the plate. The casein and isoflavone diet group was set as the control. Variation in gene expression was determined by setting the regulation threshold to 3.00.

## 2.7 Digital drop PCR (ddPCR) expression assay

### 2.7.1 RNA extraction and cDNA synthesis from adipose tissue

RNA extraction was performed according to the protocol described in Section 2.6.1. cDNA synthesis was performed using iScript cDNA Synthesis Kit (Biorad; Cat. no. 170-8890) according to the manufacturer's specifications.

### 2.7.2 RNA extraction and cDNA synthesis from 3T3-L1 cells

#### 2.7.2.1 Cell culture

The cells were grown in 100mm x 20mm plates according to the protocol outlined in Section 2.3. Protein and rosiglitazone treatments were administered at the time of differentiation (day 7) as described in Section 2.3.

#### 2.7.2.2 Trizol extraction method

On day 15, 1mL of Trizol (Invitrogen; Cat. no. 15596-018) was added to the dishes, and the cells were scraped into 1.5mL tubes. Rosiglitazone- treated cells were harvested on day 13. Cells were vortexed and sonicated for 10 seconds using the Branson Sonifier 250 (duty cycle: 60%, and output control: 1)(Danbury, CT, USA). The lysates were then centrifuged at 11 x $10^3$g for ten minutes at 4$^o$C. The upper lipid layer was removed, and the organic layer was combined with 200µL of chloroform in a new 1.5mL tube. The tubes were shaken vigorously for 15 seconds then incubated at room temperature for two minutes prior to spinning at 11 x $10^3$g for 15 minutes at 4$^o$C. The upper aqueous layer was combined with 500µL of

isopropanol and incubated for ten minutes at room temperature. The mixtures were centrifuged at 15 x $10^3$g for 15 minutes at 4°C. The supernatant was discarded and the pellets were vortexed gently with 1mL of 75% EtOH and centrifuged at 7.5 x $10^3$g for five minutes at 4°C. The supernatant was carefully removed by pipetting, and the pellets were air-dried for five minutes by inverting the tube. The dried pellets were dissolved in 75µL of $dH_2O$. The samples were incubated at 55°C for ten minutes with the caps removed in order to evaporate any remaining ethanol. Concentrations were analyzed using the NanoDrop 1000.

cDNA synthesis was performed using iScript cDNA Synthesis Kit (Biorad; Cat. no. 170-8890) according to the manufacturer's specifications.

### 2.7.3 Preparation of plasmid DNA for ddPCR optimization

Rat PPARG-ORF clone was purchased from Creative Biogene (Shirley, NY, USA; Cat. no. CDCH394852) and was cloned using an established protocol from Dr. Steve Gleddie's laboratory. Twenty-five nanograms of clone were added to a thawed aliquot of 1 x $10^6$ DH5α bacteria (Life Technologies, Cat. no. 18265-017) in 30% glycerol. The mixture was placed on ice for 30 minutes, followed by 20 seconds in a 42°C waterbath, and 2 minutes on ice again. Once cool, 960µL of Super Optimal Broth medium (Invitrogen, Burlington, ON, Canada; Cat. no. 15544-034) was added to the bacteria. The mixture was subject to agitation at 37°C for 1 hour, and a separate 20x dilution of the bacterial mixture was prepared. Two hundred microliters of the stock and 20x dilution bacterial suspensions were plated

separately onto agar (BioShop Canada Inc., Burlington, ON; Cat. no. AGR001.1) plates supplemented with 0.5ng ampicillin (BioShop Canada Inc.; Cat. no. AMP201.5), respectively. The culture was grown for 24 hours at 37°C and 5%$CO_2$. A single colony per plate was isolated and added to 5mL of LB broth (10%w/v trypton (BioShop Canada; Cat. no. TRP 402), 5% w/v yeast extract (BioShop Canada; Cat. no. YEX 401), and 10%w/v NaCl) supplemented with 0.5ng ampicillin. Suspension colonies were grown overnight at 37°C with constant agitation.

In preparation for RNA extraction, 500µL of the suspension culture was spun at maximum speed for 5 minutes. The pellet was collected and used for RNA extractions using the protocol described in Section 2.3.1.

### 2.7.4 ddPCR analysis

The peroxisome proliferator- activated receptor γ *(pparγ)* primer (isoform non-specific) was purchased from Qiagen (Cat. no. PPR47599A-200). Primers for β-2 microglobulin *(b2m)*, lactate dehydrogenase *(ldha)*, and uncoupling protein-1 *(ucp-1)* were purchased from Qiagen (Cat. nos. PPR42607A-200, PPR56603B-200, PPR44766A-200, respectively).

Based on the results from the adipogenesis array, expression of PPARγ and UCP-1 were quantified in male and female rat adipose cDNA. Concentration optimization was performed using a concentration gradient (0.4pg to 2pg) of the PPARG-ORF clone. Temperature optimization was performed using the PPARG-ORF clone and an annealing temperature gradient (53°C to 63°C).

Eight biological repetitions were used for the rat tissue samples; six biological repetitions were used for the 3T3-L1 samples.

PCR reactions were prepared in 96-well PCR plates, with each well containing the following: 5µL of 0.2ng/µL sample, 12.5µL of 2X QX200™ ddPCR EvaGreen Supermix (Biorad; Cat. no. 186-4034), 0.25µL of 10µM primer, and 7.25µL of $dH_2O$. Plates were centrifuged at 200g for 1 minute, and 20µL of each reaction mix was transferred to DG8™ Cartridges (Biorad; Cat. no. 186-4008). Seventy microlitres of QX200™ Droplet Generation Oil for EvaGreen (Biorad; Cat. no. 186-3305) was added to a separate well on the cartridge, and the cartridge was passed through the QX200™ Droplet Generator (Biorad; Cat. no. 186-4002). Forty microlitres of the final product was transferred into a Twin-Tec 96-well plate (Eppendorf, Missisauga, ON, Canada; Cat. no. 951-020-303) and sealed using Pierceable Foil Heat Seal (Biorad; Cat. no. 181-4040) and PX1™ PCR Plate Sealer (Biorad; Cat. no. 181-4000). PCR amplification was performed on the C1000 Touch™ Thermal Cycler according to the following protocol: hot start activation at 95°C for 10 minutes, 45 cycles of 30 seconds at 95°C and one minute at 59°C, followed by 10 minutes at 98°C. Quantification of PCR reaction was performed using the QX200™ Droplet Reader (Biorad 186-4003) and Quantasoft 1.6.6 software.

### 2.7.5 Statistical analysis

Sample concentrations determined by Quantasoft software were used to determine fold differences. The sample concentrations for each target gene were

normalized using the geometric means of lactate dehydrogenase A (*ldha*) and β-2 microglobulin (*b2m)* mRNA sample concentrations. Fold difference was calculated by dividing the normalized concentrations by the control concentration. Outliers were determined using the Modified Thompson τ method. Statistical significance was defined as $p<0.05$ and was determined by one-way ANOVA and Fisher LSD analysis using SigmaPlot 12.5.

## 2.8 Protein analysis

### 2.8.1 Protein extraction and quantification from adipose tissue

Approximately 500mg of frozen adipose tissue was collected per animal, and mixed with 500µL of Frack's buffer (20 mM Tris pH 7.5, 150 mM NaCl, 2 mM EDTA pH 8.0) supplemented with 2 mM NaF, 2 mM NaPP, 500 µM $Na_3VO_4$, 200 µg/ml PMSF, 2µg/ml aprotinin, 2 µg/ml leupeptin (Roche cOmplete Mini EDTA-free Protease Inhibitor Cocktail Tablets; Laval, QC, Canada; Cat. no. 04693159001). Tissues were then homogenized for 10 seconds on ice using the Polytron PT 3100 (Kinematica; Bohemia, NY, USA) and sonicated for 10 seconds. Samples were centrifuged at approximately 12,000g for 20 minutes at 4oC. The pink lower layer was retained and stored at -80oC for further use.

Protein quantification was measured using the DCTM Protein Assay (Biorad; Cat. nos. 500-0113, 500-0114, 500-0115) according to the manufacturer's recommendations with the following modifications: stock solutions were diluted to 1:2 working solutions, and 1µL of the dilutions was used for the quantification

assay. For each sample, 50µL of A' working solution and 400µL of Reagent B was added. The mixtures sat at room temperature for 15 minutes, and were transferred to a 96-well plate for absorbance reading at 655nm. Protein concentrations were determined using Prism 3.0 software. Bovine serum albumin standard (Thermo Scientific; Cat. no. 23209) was used to create a standard curve for each quantification experiment.

### 2.8.2 Protein extraction and quantification from 3T3-L1 cells

Mouse preadipocytes (3T3-L1) (ATCC CL-173™) were seeded at a density of 2.0 x $10^4$ cell/mL onto 60mm x 15mm plates in 10mL of growth media. Cells were grown for seven days at 37°C and 5% $CO_2$ with the media being replaced every 48 hours. On day 7 or 8, cells were incubated in 5mL of differentiation media and 200µM sterile-filtered casein or soy protein dissolved in $dH_2O$ (for information on the protein refer to Section 2.1.2). Rosiglitazone (6µM) was used as a positive control.

On day 15 or 16, media was removed and the cells were rinsed with 2mL of 1X PBS. Rosiglitazone-treated cells were harvested on day 13. Dishes were placed on ice, and cells were incubated with 300µL of chilled Frack's buffer for 30 seconds. Cells were scraped off the dish and collected in a 1.5mL centrifuge tube. The cell lysates were vortexed for 30 seconds and sonicated for ten seconds. Following cell disruption, the lysates were centrifuged at 13 x $10^3$g for 20 minutes at 4°C. The lower phase was collected and stored at -80°C until further use.

Protein quantification was performed according to the protocol highlighted in Section 2.8.1.

### 2.8.3 Western blot analysis

The Western blotting protocol was obtained from Dr. Xiao's lab (Health Canada). Using the protein quantification data, 50µg of protein were combined with 7.5µL of 4X loading buffer (200 mM Tris.Cl pH 6.8, 400 mM DTT, 8% SDS, 0.4% bromophenol blue, and 40% glycerol) and Frack's buffer up to 30µL. Protein preparations were boiled in a humid bath at 100°C for three minutes then chilled on ice for five minutes. Samples were loaded onto Criterion TGX Stain-Free gels (Biorad; Cat. no. 567-8104) and run at 110 volts for 1.5 hours in 1X SDS running buffer (250 mM Tris, 1.92 M glycine, 1% SDS). Precision Plus Protein Dual Standards SDS-PAGE standard (Biorad; Cat. no. 1610374) and Precision Plus Low Range standard (Biorad; Cat. no. 1610305) were used.

Gels were activated for one minute using the Chemidoc MP Imaging system (Biorad; Cat. no. 170-8280) then transferred onto PVDF membranes for one hour at 50 volts in transfer buffer (25 mM Tris, 0.192 M glycine, 20% methanol). Total transferred protein was imaged using a one minute exposure of the membrane on the Chemidoc MP Imaging system. The membrane was then incubated for one hour at room temperature (approximately 24°C) with constant agitation in a blocking buffer (15 mM NaCl, 1 mM Tris.-Cl (pH 8.0), 0.1% Tween-20 (TBST), and 5% skim milk powder (Bulk Barn, Ottawa, ON, Canada)). A 1:500 dilution of PPARγ (Cell Signalling, Beverly, MA, USA; Cat. no. 2443) was prepared in 5% w/v BSA, 1X TBS,

and 0.1% TBS. A 1:500 dilution of UCP-1 (Abcam, Cambridge, MA, USA; Cat. no. 10983) was prepared in blocking buffer. A 1:1000 dilution of β actin (Abcam; Cat. no. ab8227) was prepared in blocking buffer. Membranes were incubated in primary antibody overnight at 4$^{o}$C with constant agitation. Following this, the membranes were washed twice for seven minutes in TBST and incubated in secondary antibody for one hour at room temperature with constant agitation. The secondary antibody and any background binding were removed with three sets of ten minute washes in TBST with constant agitation. Bands were detected using a 1:1 dilution of the Super Signal West Femto Maximum Sensitivity kit) or Dura Enhanced Chemiluminescence kit (Thermo Scientific; Cat. nos. 34095 and 34075). Membranes were imaged on the Chemidoc MP Imaging system.

### 2.8.4 Statistical analysis

Densitometric analysis of band intensity was conducted using Image Lab 5.1 software. Background detection was removed, and bands were normalized against their counterpart β-actin bands. Fold differences were calculated by dividing the normalized volumes by the data for the control treatment. Outliers were determined using the Modified Thompson τ method. Statistical significance was defined as $p<0.05$ and was determined by one-way ANOVA and Fisher LSD analysis using SigmaPlot 12.5.

# 3 CHAPTER: RESULTS

## 3.1 Soy-dependent changes in 3T3-L1 morphology

### 3.1.1 Visual observation of 3T3-L1 morphology

An optimal treatment concentration was determined for rosiglitazone, which served as a positive control. The optimal concentration was determined based on visual observations of the amount of cell sloughing and microscopic analysis of intracellular lipid accumulation. All treatments lower than 6μM showed little cell sloughing but little adipocyte maturation and lipid accumulation (Figure 3.1 A, B, C, & D). The 8μM treatment showed substantial cell sloughing (Figure 3.1 F). The 6μM treatment showed almost 100% cell differentiation and lipid accumulation with minimal cell sloughing (Figure 3.1 E). This was chosen as the optimal concentration for rosiglitazone treatments for future experiments

A similar optimization experiment was performed to determine the treatment concentration of the protein hydrolysate samples. The optimal concentration was determined based on lipid accumulation in the casein experiment and was supported using the Harovinton experiment. There was low lipid accumulation in the 50μg/mL and 100μg/mL treatments, suggesting insufficient levels of casein in the growth media (Figure 3.2 A & B). The 400μg/mL casein treatment appeared to hinder differentiation, indicating that this concentration might be toxic to the cells. Therefore, 200μg/mL was chosen as the optimal protein treatment concentration for future experiments.

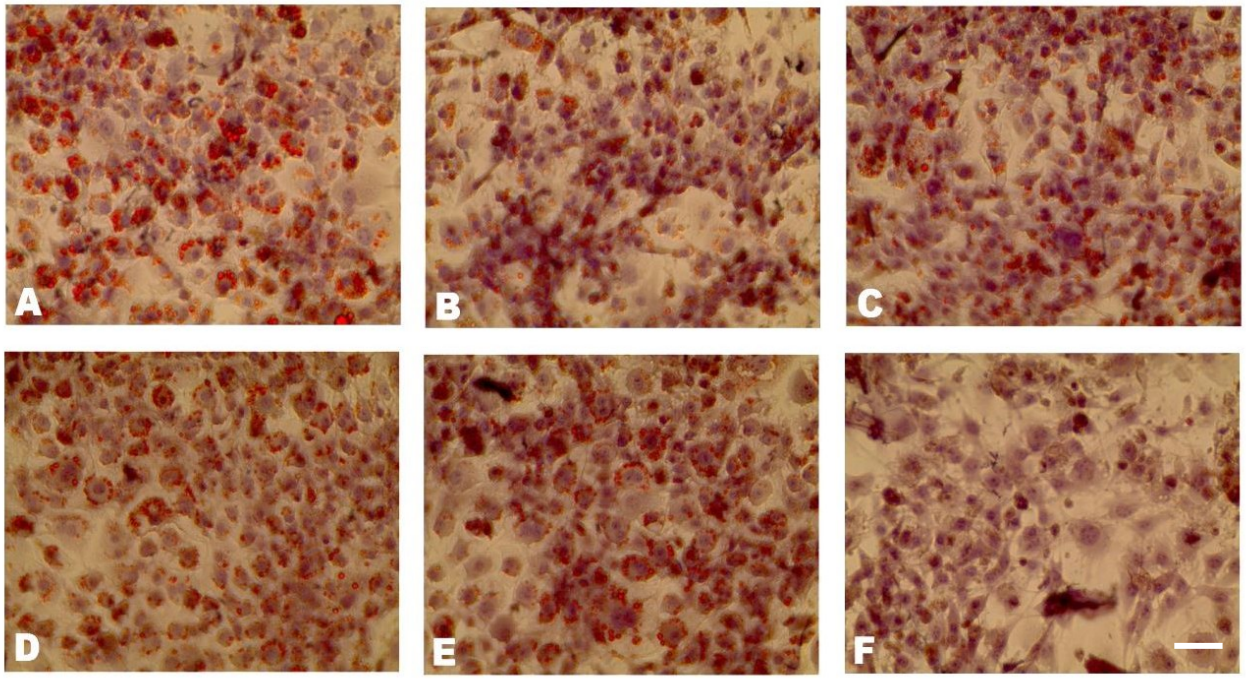


**Figure 3.1.** Mouse 3T3-L1 cells treated with different concentrations of rosiglitazone at the time of differentiation. Rosiglitazone dissolved in DMSO was provided to cells at the following concentrations: A- 0μM, B- 1μM, C- 2μM, D- 4μM, E- 6μM, F- 8μM. Cells were differentiated on day 7 and stained on day 15. Lipids were stained with Oil Red O, and hematoxylin was used as a counterstain. Cells were visualized with bright field microscopy on the EVOS microscope. Images are representative of three replicates. Scale bar represents 300μm.

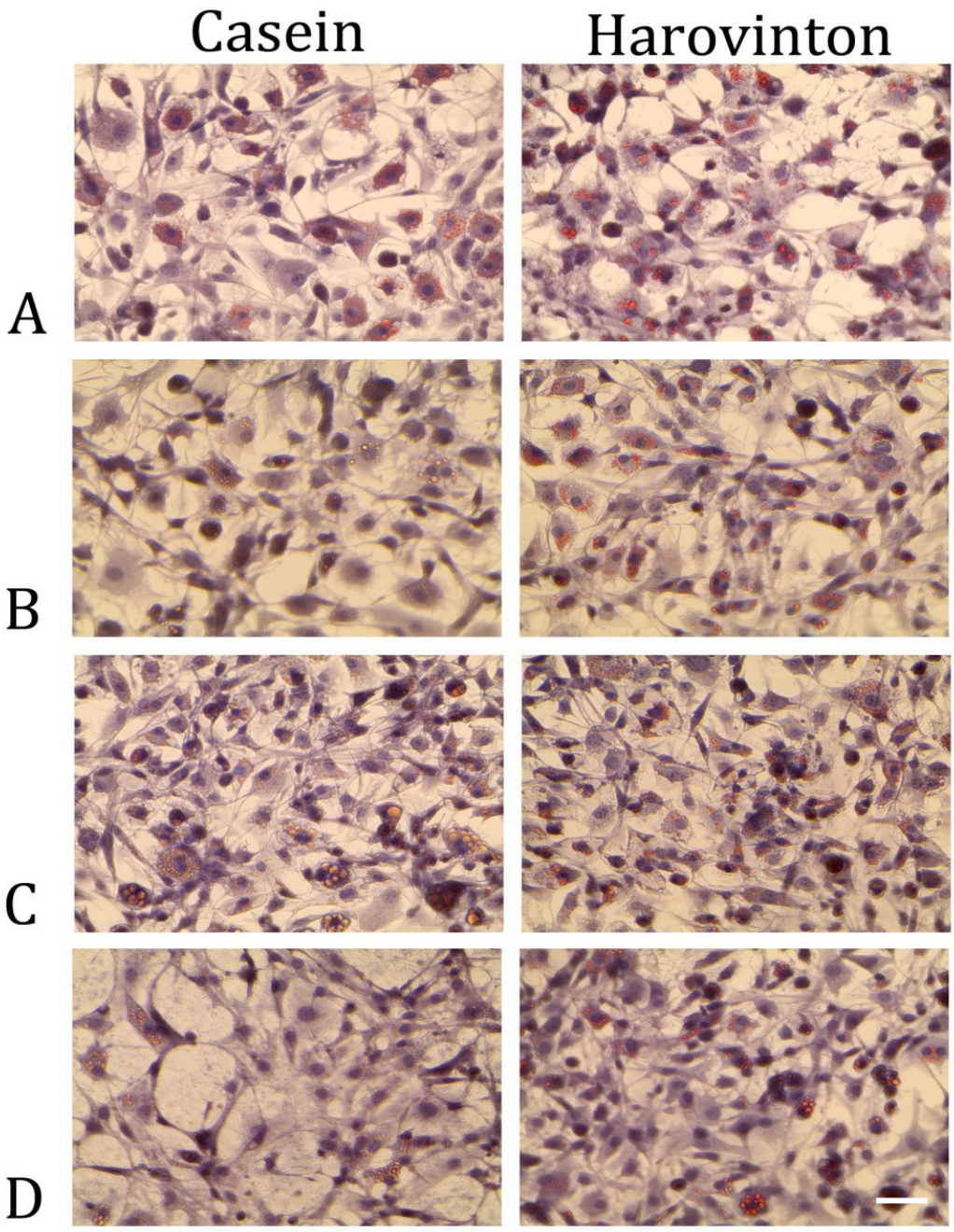


**Figure 3.2.** Mouse 3T3-L1 cells treated with different concentrations of casein and Harovinton at the time of differentiation. Protein hydrolysates dissolved in water were provided to cells at the following concentrations: Row A- 50µg/mL, Row B- 100µg/mL, Row C- 200µg/mL, Row D- 400µg/mL. Cells were differentiated on day 7 and stained on day 15. Lipids were stained with Oil Red O, and hematoxylin was used as a counterstain. Cells were visualized with bright field microscopy on the EVOS microscope. Images are representative of three replicates. Scale bar represents 300µm.

Once the optimal treatment concentrations were established, mouse 3T3-L1 cells were differentiated in the presence of soy protein, and the lipids droplets were stained with Oil Red O. The droplets were visually observed and measured, and the lipid content of the mature cells was measured.

No differences in differentiation or lipid accumulation were observed in mouse 3T3-L1 cells treated with soy protein at the time of differentiation or 48 hours later. For both treatment time-points, untreated cells presented almost complete population differentiation, and lipids were stored in droplets of varying sizes (Figures 3.3A & 3.4A). The other cell treatment groups also presented almost complete population differentiation; however there were slight differences in lipid accumulation. Rosiglitazone-treated cells appeared to store lipids in very small droplets relative to the No Treatment control group (Figures 3.3B & 3.4B). Casein or Harovinton treatments did not appear to alter lipid accumulation in relation to the No Treatment control (Figures 3.3C and D & 3.4C and D). Cells treated with 1a hydrolysates were the most morphologically different of all the treatment groups in terms of lipid storage. These cells stored lipids in very large droplets in comparison to all the other treatment conditions (Figures 3.3E & 3.4E).

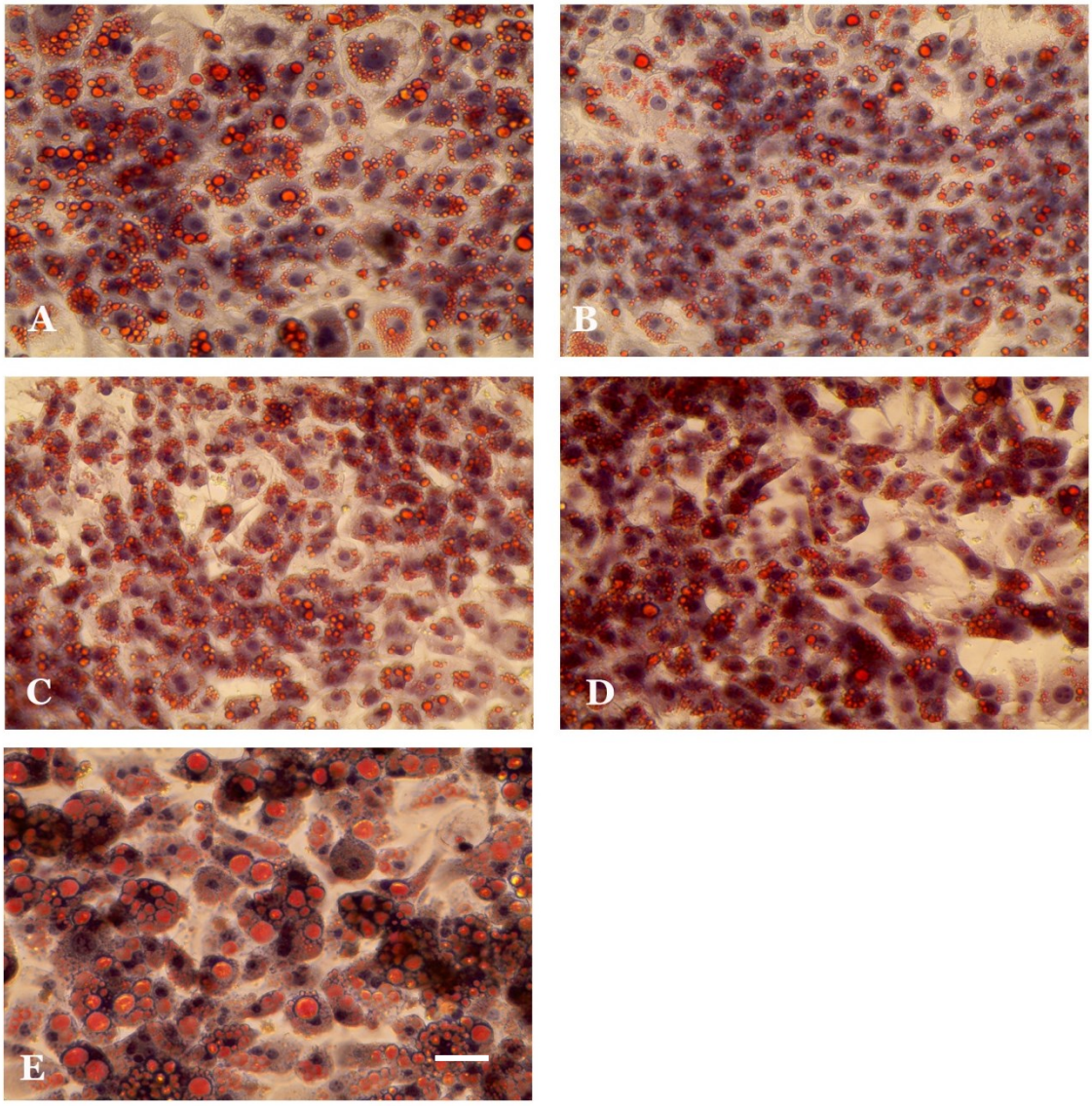


**Figure 3.3.** Lipid droplets of 3T3-L1 (ATCC CL-173) following protein treatments at the time of differentiation. Panels represent the following treatments: A- No treatment control, B- Rosiglitazone (6μM), C- Casein, D- Harovinton, E- 1a. Cells were differentiated in the presence of either protein (200μg/well) or rosiglitazone (6μM) treatments and stained on day 15. Lipids were stained with Oil Red O, and hematoxylin was used as a counterstain. Note that Panel E shows yellow droplets due to intracellular acidity; the experimental results are still valid. Cells were visualized with bright field microscopy on the EVOS microscope. Images are representative of six replicates. Scale bar represents 300μm.

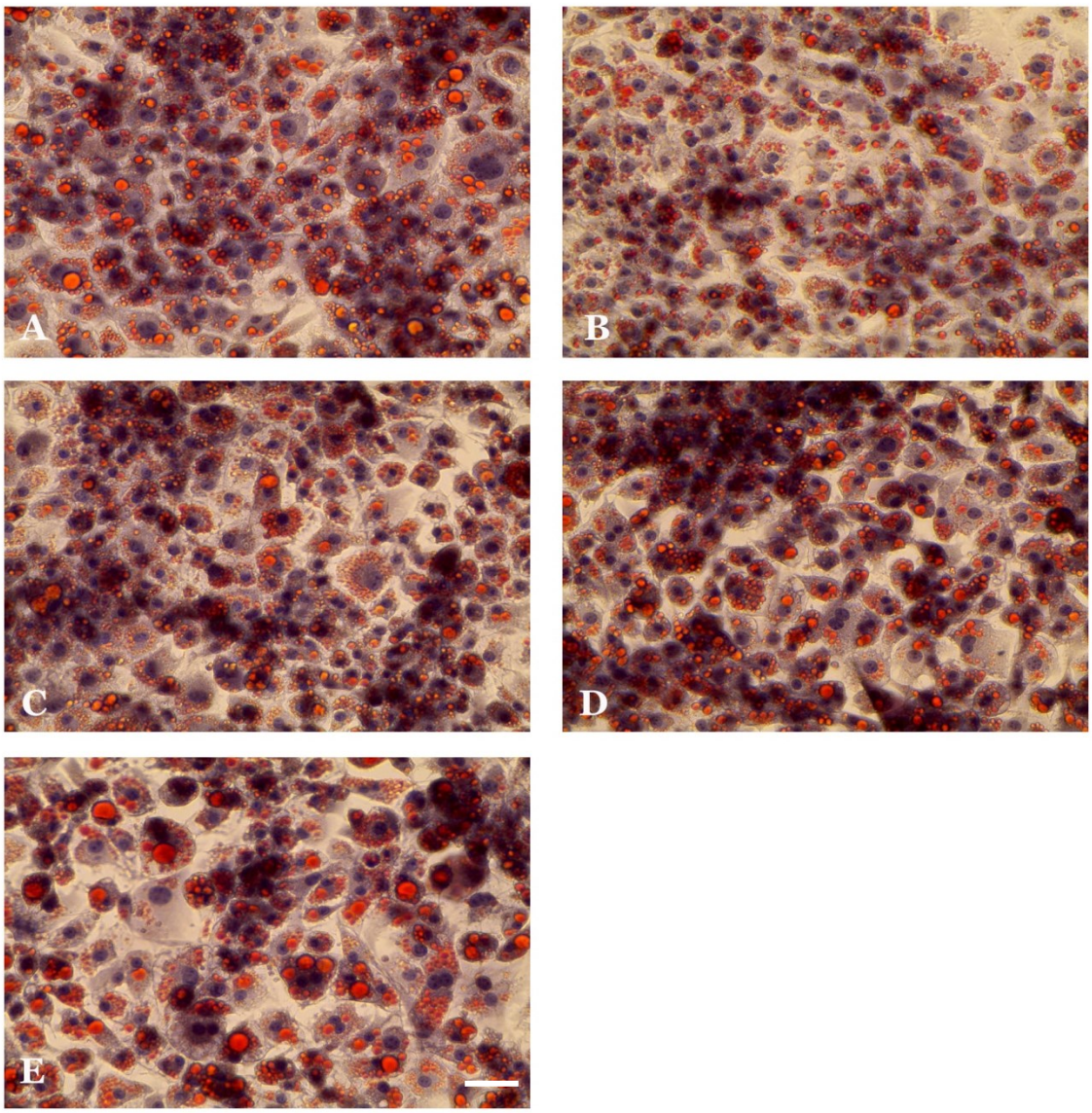


**Figure 3.4.** Lipid droplets of 3T3-L1 (ATCC CL-173) following protein treatments administered 48 hours after the time of differentiation. Panels represent the following treatments: A- No treatment control, B- Rosiglitazone (6µM), C- Casein, D- Harovinton, E- 1a. Cells were differentiated on day 7, treated with either protein (200µg/well) or rosiglitazone (6µM) treatments on day 9, and stained on day 15. Lipids were stained with Oil Red O, and hematoxylin was used as a counterstain. Cells were visualized with bright field microscopy on the EVOS microscope. Images are representative of six replicates. Scale bar represents 300µm.

### 3.1.2 Lipid droplet measurements

As a follow-up to visual observation of lipid accumulation, lipid droplet areas were measured using Northern Eclipse 1.0 software and were graphed according to size for both treatment time points. For both treatment time points, an inverse relationship was observed between the size and the number of lipid droplets (Figure 3.5 & Figure **3.6**). Mouse 3T3-L1 cells appeared to preferentially store cells in smaller droplets when treated with rosiglitazone and most protein hydrolysates. Notably, in each treatment group, a small increase in the number of very large lipid droplets (≥ 0.1mm$^2$) was observed. Treatment of mouse 3T3-L1 cells with casein, Harovinton, or 1a hydrolysates seemed to result in a similar droplet percent distribution when compared to the No Treatment control.

When cells were treated at the time of differentiation, Fisher LSD analysis revealed significant differences in certain droplet size categories. Cells treated with Harovinton hydrolysates stored lipids in smaller droplets (0.005 to 0.01mm$^2$) when compared to cells treated with either casein or 1a protein hydrolysates ($p<0.02$). Cells treated with 1a hydrolysates showed an affinity towards storing lipids in larger droplets, evidenced by the higher percentage of 0.055-0.06mm$^2$ and ≥0.1mm$^2$ droplets ($p<0.01$, $p<0.001$). This result was in agreement with the large droplets that were observed in the 1a-treated cells in Section 3.1.1.

Administration of protein treatments 48 hours after differentiation revealed very similar results, with 1a hydrolysate-treated cells preferentially storing lipids in larger droplets; however these results were not statistically significant (Figure 3.6).

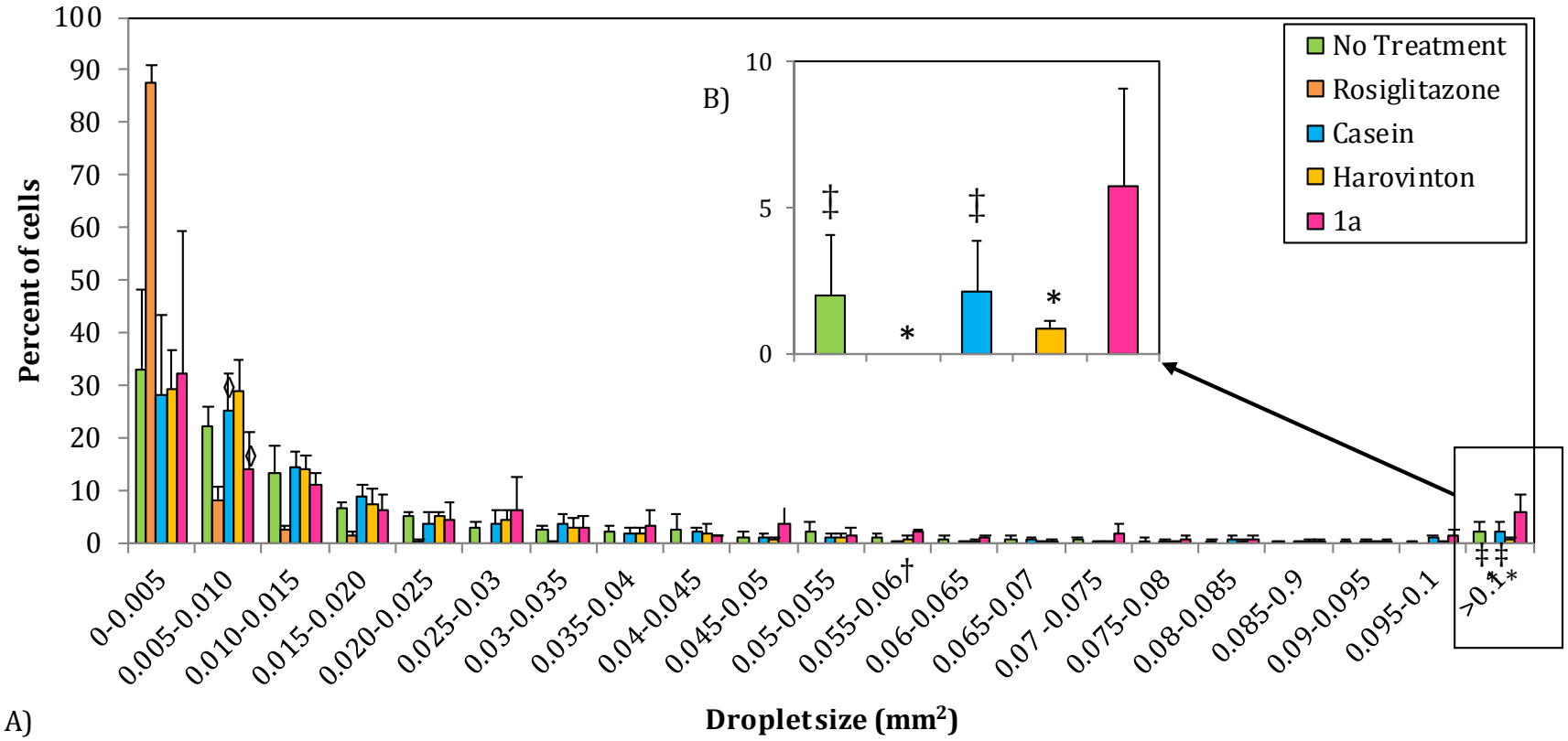


**Figure 3.5**. Size distribution of lipid droplets in 3T3-L1 adipocytes treated with soy protein hydrolysates at time of differentiation. A- Full range of size distribution. B- Magnified view of the > 0.1 droplet size group. Cells were differentiated in the presence of either protein hydrolysates (200µg/well) or rosiglitazone (6µM), and droplet areas were calculated using Northern Eclipse 1.0 software. Values are mean percentages of droplet populations ± SD (n=6). Significance was determined by one-way ANOVA and Fisher LSD analysis: ◊ *p<0.02 versus Harovinton (0.005-0.010mm²), † p<0.008 versus 1a (0.005-0.060mm²), ‡ p<0.01 versus 1a (≥0.1mm²), *p≤0.001 versus 1a (≥0.1mm²).*

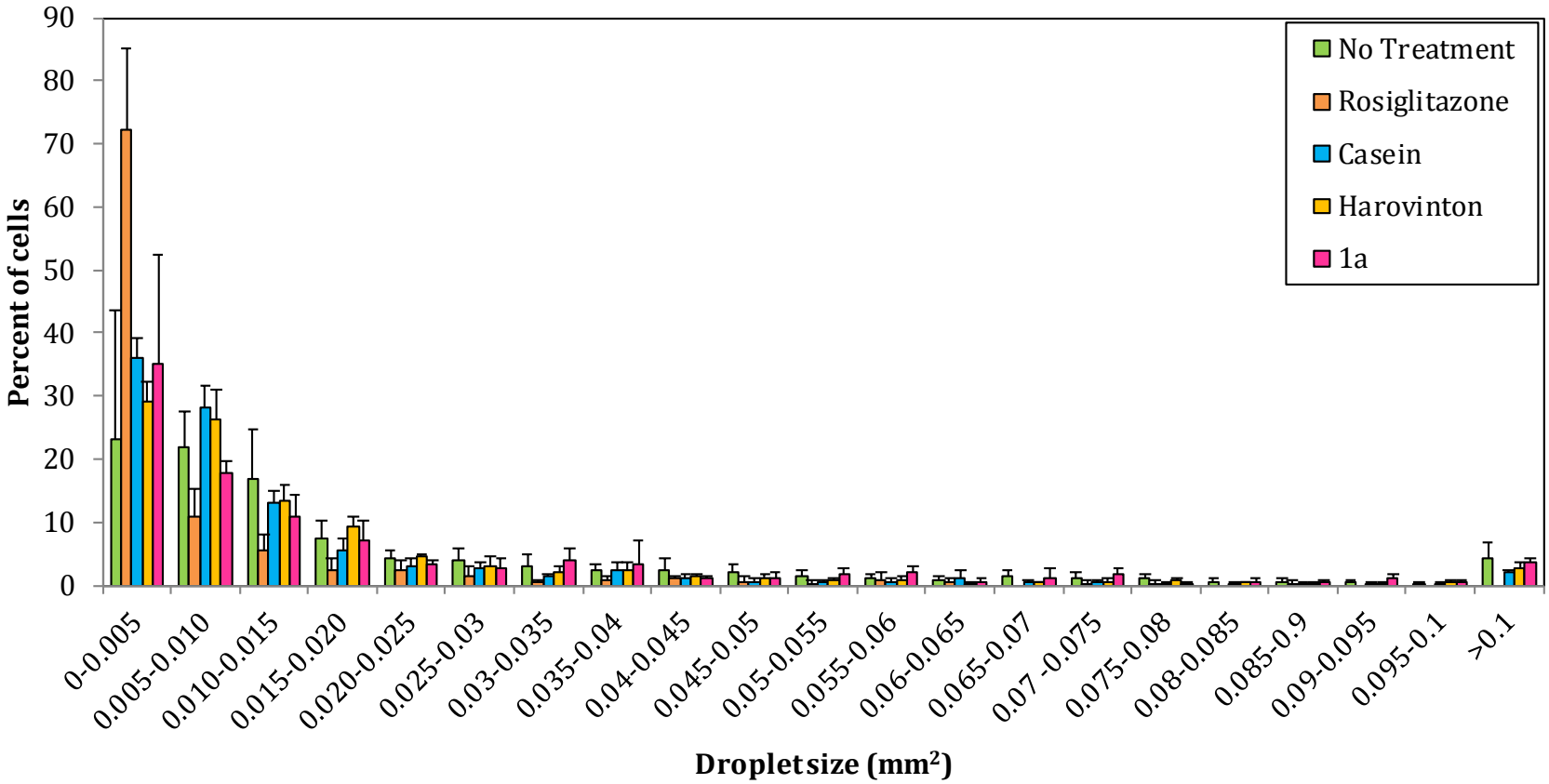


**Figure 3.6**. Size distribution of lipid droplets in 3T3-L1 adipocytes treated with soy protein hydrolysates 48 hours after the time of differentiation. Cells were differentiated in the presence of either protein hydrolysates (200µg/well) or rosiglitazone (6µM), and droplet areas were calculated using Northern Eclipse 1.0 software. Values are mean percentages of droplet populations ± SD (n=6). No significance was determined using one-way ANOVA analysis.

### 3.1.3 Quantification of lipid accumulation

Stored lipids were also quantified in 3T3-L1 cells. Lipid-staining Oil Red O dye was extracted, and the concentration was determined using absorbance measurements. Data was normalized by the total number of cells in each well determined using Hoescht fluorescence absorbance. All the absorbance values were represented as fold differences compared to the No Treatment condition (control condition), which was set to a value of one. The quantification assay was only performed on cells treated with protein hydrolysates at the time of differentiation because no significant differences in lipid droplet size was observed when cells were treated with protein 48 hours after differentiation (Figure 3.6).

As expected, cells treated with rosiglitazone showed the greatest change in lipid accumulation relative to all the other treatment groups, with a 1.5-fold increase in lipid accumulation compared to the control (Figure 3.7). Cells treated with casein stored 0.9-fold less lipids in relation to the control and had significantly less lipid accumulation in relation to the rosiglitazone treatment group ($p<0.007$). Although not significantly difference, both soy hydroloysate treatment groups did exhibit higher levels of lipid accumulation than the control and casein treatment groups. Cells treated with Harovinton hydrolysates presented no change in fold difference relative to the control, whereas cells treated with 1a hydrolysates presented a 1.15-fold increase in lipid accumulation relative to the control. The Fisher LSD analysis method did not identify the comparisons between the casein, Harovinton, and 1a treatment groups as being statistically significant.

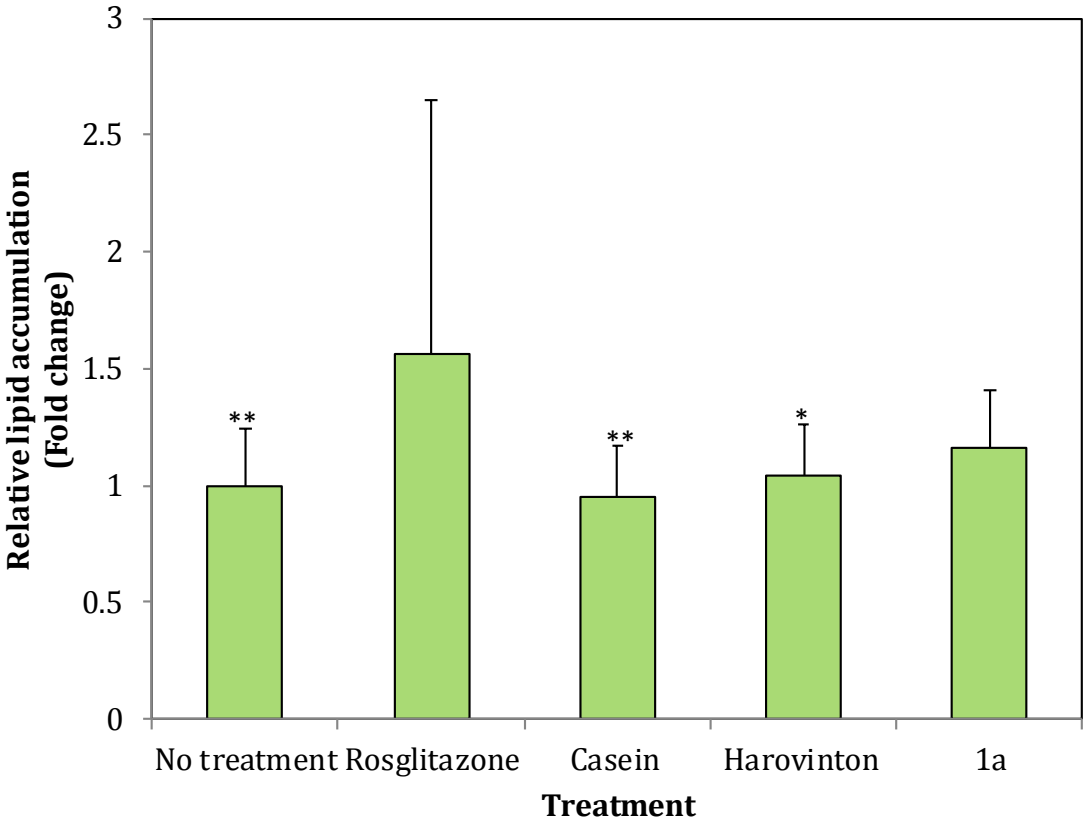


**Figure 3.7.** Lipid accumulation in mouse 3T3-L1 cells following treatments (protein 200µg/mL, rosiglitazone 6µM) at the time of differentiation. Lipids were stained with Oil Red O and dye absorbance was measured at 492nm. Nuclei were stained with Hoescht, and fluorescence readings (ex. 353nm, em. 483nm) were used to normalize the data. Values are mean fold differences relative to the No Treatment group ± SD (n=14). One-way ANOVA and Fisher LSD analysis revealed significant pairwise comparisons: ** p<0.02 versus rosiglitazone, ** p<0.007 versus rosiglitazone*.

## 3.2 Soy-dependent changes in mRNA expression of PPARγ and UCP-1

Previous *in vivo* studies demonstrated reductions in body fat content upon consumption of soy protein (Chen et al, 2014); therefore, changes in adipogenic gene expression in rats fed soy-supplemented diets were explored.

### 3.2.1 Adipogenesis array

Male rat adipose RNA samples were analyzed using adipogenesis qPCR array plates. Gene expression was graphically presented as a delta delta Ct value to highlight gene abundance. The casein and isoflavone diet was set as the baseline expression profile since the Harovinton and 1a diets both contained isoflavones. For the three soy diets (SPI, Harovinton, and 1a), *pparγ* expression levels did not show any change in comparison to the baseline ($p>0.05$).

The adipogenesis array did reveal gene expression changes for *ucp-1* across the different diets (

Figure 3.8). In comparison to the casein and isoflavone control, *ucp-1* gene expression appeared to be up-regulated six-fold in rats that were fed SPI and three-fold in rats fed Harovinton. Rats fed Diet 1a did not exhibit any changes to *ucp-1* gene expression relative to the control. The observed trends for both male and female samples were not significant ($p=0.1$).

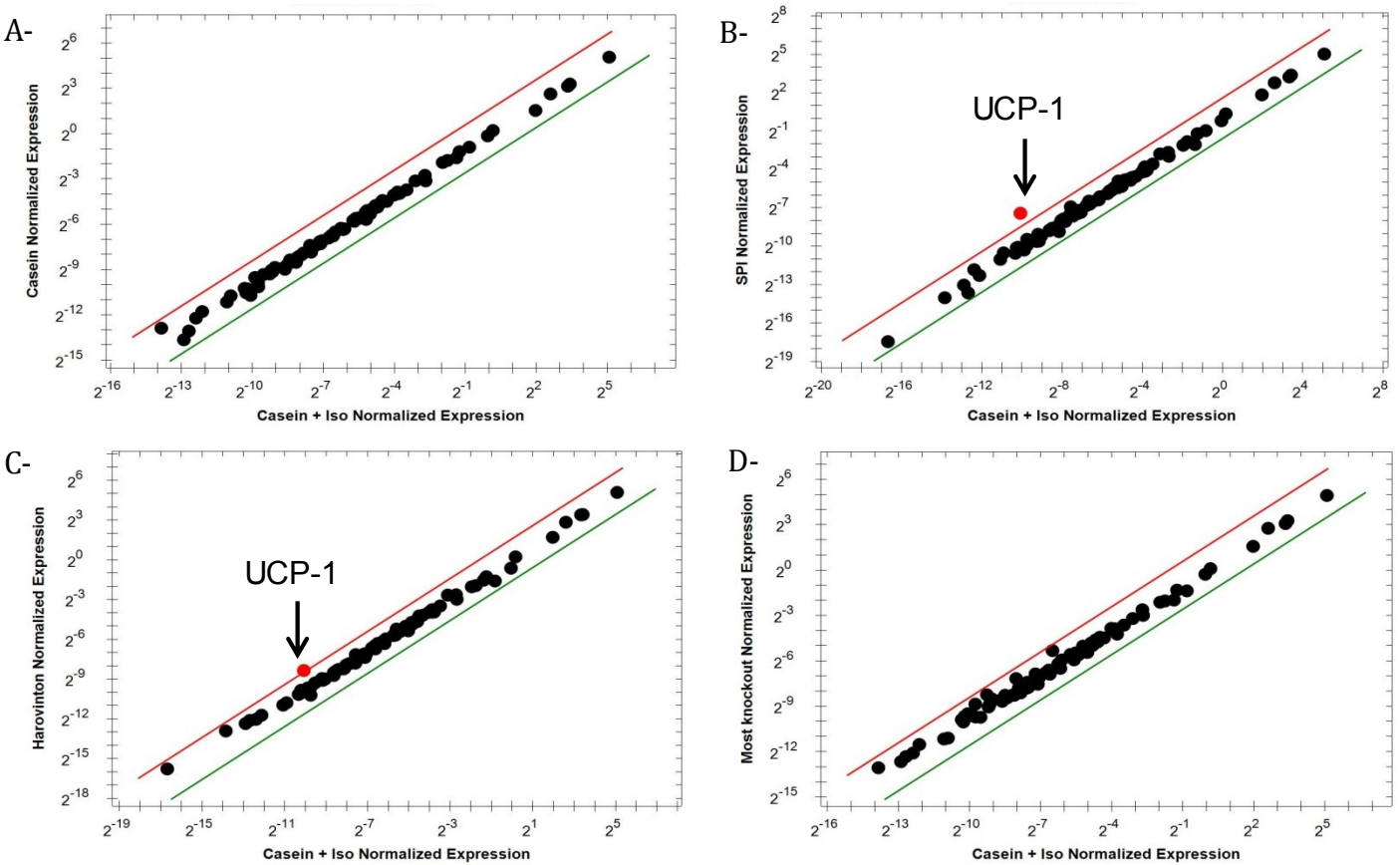


**Figure 3.8**. Expression change of adipogenic genes in male rat adipose tissue as a result of soy diets in comparison with a casein and isoflavone diet. RNA was extracted from adipose tissue of the rats fed diets containing 20-30% protein, and relative expression for each diet was determined: A- Casein, B- Soy protein isolate (SPI), C- Harovinton, and D- 1a (Most knockout). qPCR analysis was performed using RT$^2$ Rat Adipogenesis Profiler Array, and data was analyzed using CFX Manager 3.1 software. Black dots represent all the genes that showed no expression change with respect to the control. Red dots indicate up-regulated uncoupling protein 1 (*ucp-1*) gene expression with respect to the control. N= 5.

### 3.2.2 *In vivo* ddPCR experiment

The results of the adipogenesis microarray did not provide any evidence that *pparγ* gene expression levels varied in response to protein treatments. In these analyses, the cycle threshold values of the *pparγ* gene were higher than optimal (Ct<29), which suggests that there may be very little *pparγ* mRNA in the samples. Consequently, male and female adipose tissue RNA samples were were re- analyzed using Digital drop PCR (ddPCR). RNA was extracted using a Trizol method to improve product yield instead of the RNEasy kit that was used for the adipogenesis array. Uncoupling protein- 1 gene expression was also tested using ddPCR. Both target genes were normalized using *ldha* and *b2m* gene expression. Fold differences were calculated using the casein and isoflavone diet as the control.

Overall, very little change in *pparγ* gene expression was observed between the male diet groups. There was a slight decrease in expression in the casein diet group relative to the control group; however, this difference was not statistically significant (p=0.9).

Sex-related differences were noted when considering the diet groups (p<0.002) (Figure 3.9). The female rats showed a much higher overall *pparγ* gene expression than their male counterparts. In contrast to the trend observed in the male rats, there appeared to be a slight increase in *pparγ* gene expression in female rats fed casein in relation to the control (p=0.5). Moreover, gene expression of *pparγ* appeared to be higher in the Harovinton diet group than all the other diet

groups (p=0.01 vs SPI, p=0.03 vs 1a, p=0.08 vs casein, p=0.5 vs casein and isoflavones). The 1a diet group seemed to exhibit the lowest *pparγ* expression comparative to the other soy diet groups (p=0.7 vs casein, p=0.7 vs casein and isoflavones, p=0.1 vs SPI, p=0.03 vs Harovinton).

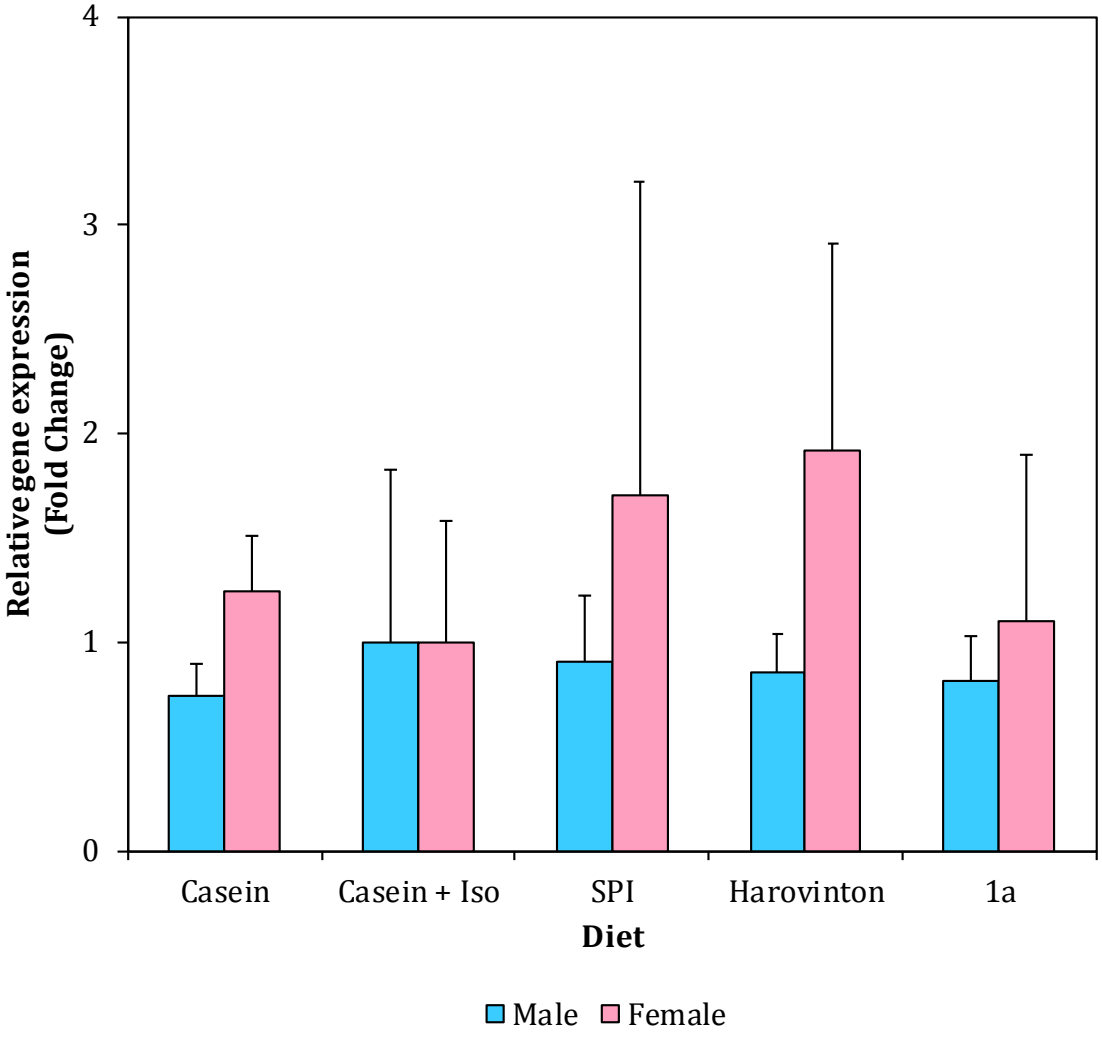


**Figure 3.9.** Gene expression of adipose peroxisome proliferator- activated receptor γ *(pparγ)* in male and female rats fed diets containing 20% protein. Adipose mRNA was analyzed using Digital drop PCR. Values are mean fold differences compared to the casein and isoflavone treatment group ± SEM (baseline=1; n=8). Two-way ANOVA revealed sex-related differences ($p \leq 0.002$).

Digital drop PCR analysis did not reveal any sex-related differences in *ucp-1* expression. The male and female samples were therefore combined to obtain overall *ucp-1* expression results. One-way ANOVA and Fisher LSD analysis was used to determine significance. Fold differences of expression were calculated using the casein and isoflavone group as the control (baseline set to 1).

There was a pronounced decrease in *ucp-1* expression in the casein diet group compared to the control, indicative of a possible isoflavone effect ($p<0.001$) (Figure 3.10). Similarly, there was an observed decrease in *ucp-1* expression in the rats fed SPI or Harovinton hydrolysates relative to the control ($p<0.001$). Rats fed 1a hydrolysates exhibited similar *ucp-1* expression compared to the control. The 1a diet group also exhibited significantly elevated *ucp-1* expression levels relative to the casein, SPI, or Harovinton diet groups ($p<0.001$).

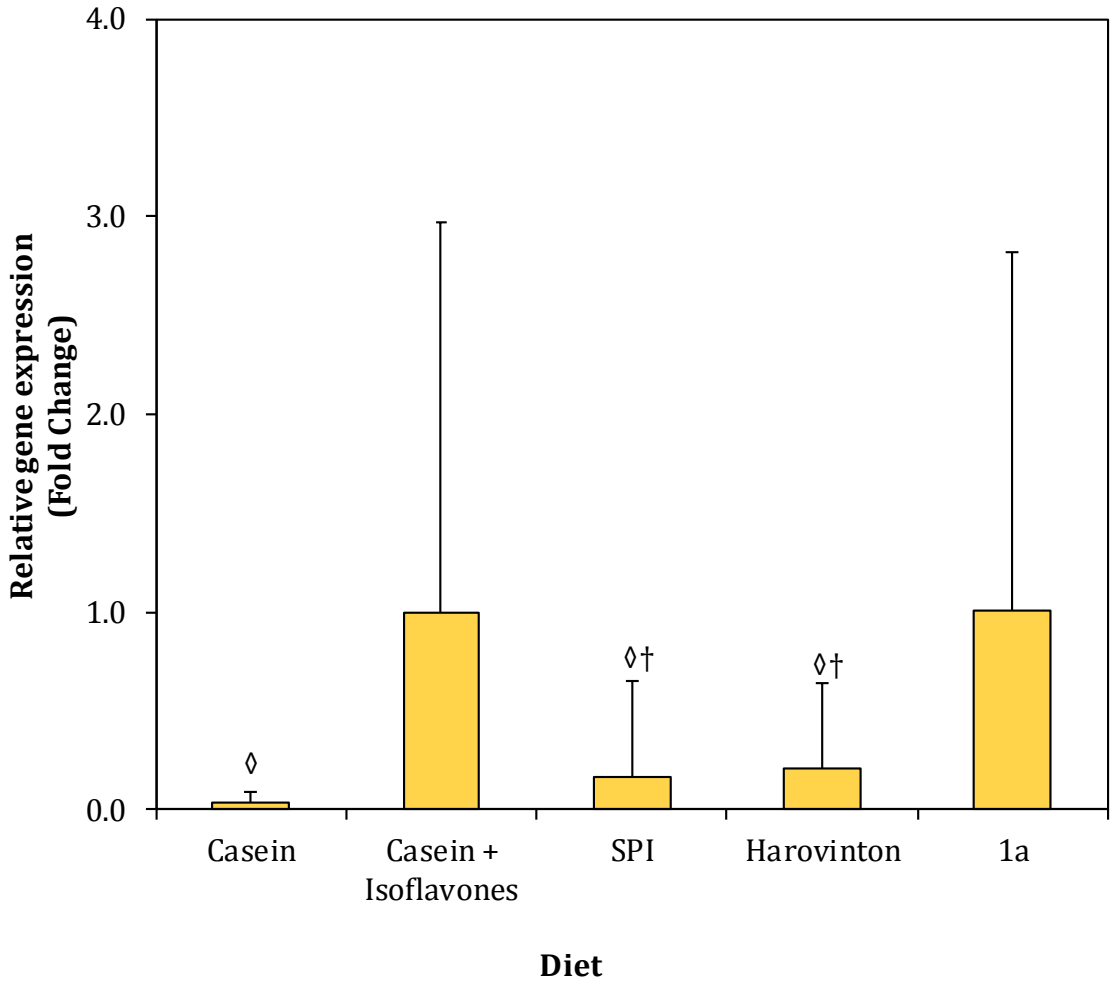


**Figure 3.10.** Gene expression levels of adipose uncoupling protein 1 *(ucp-1)* in rats fed diets containing 20% protein. Adipose mRNA was analyzed using Digital drop PCR. Values are mean fold differences compared to the casein and isoflavone treatment group ± SEM (baseline=1; n=16). One-way ANOVA and Fisher LSD analysis revealed statistical significance: ◊ *p<0.001 versus Casein + Isoflavones,* † *p<0.001 versus 1a*.

### 3.2.3 *In vitro* ddPCR experiment

To complement the *in vivo* experiment, RNA from 3T3-L1 cells differentiated with protein treatments was extracted and analyzed using ddPCR using *ldha* and *b2m* gene expression levels to normalize the results. Fold differences were calculated using the casein and isoflavone diet as the control.

No statistically significant differences were observed between the treatments; however a few trends were observed. The Harovinton treatment did not appear to alter PPARγ expression. The casein and 1a treatments appeared to decrease PPARγ expression by half in comparison to the control and Harovinton treatments.

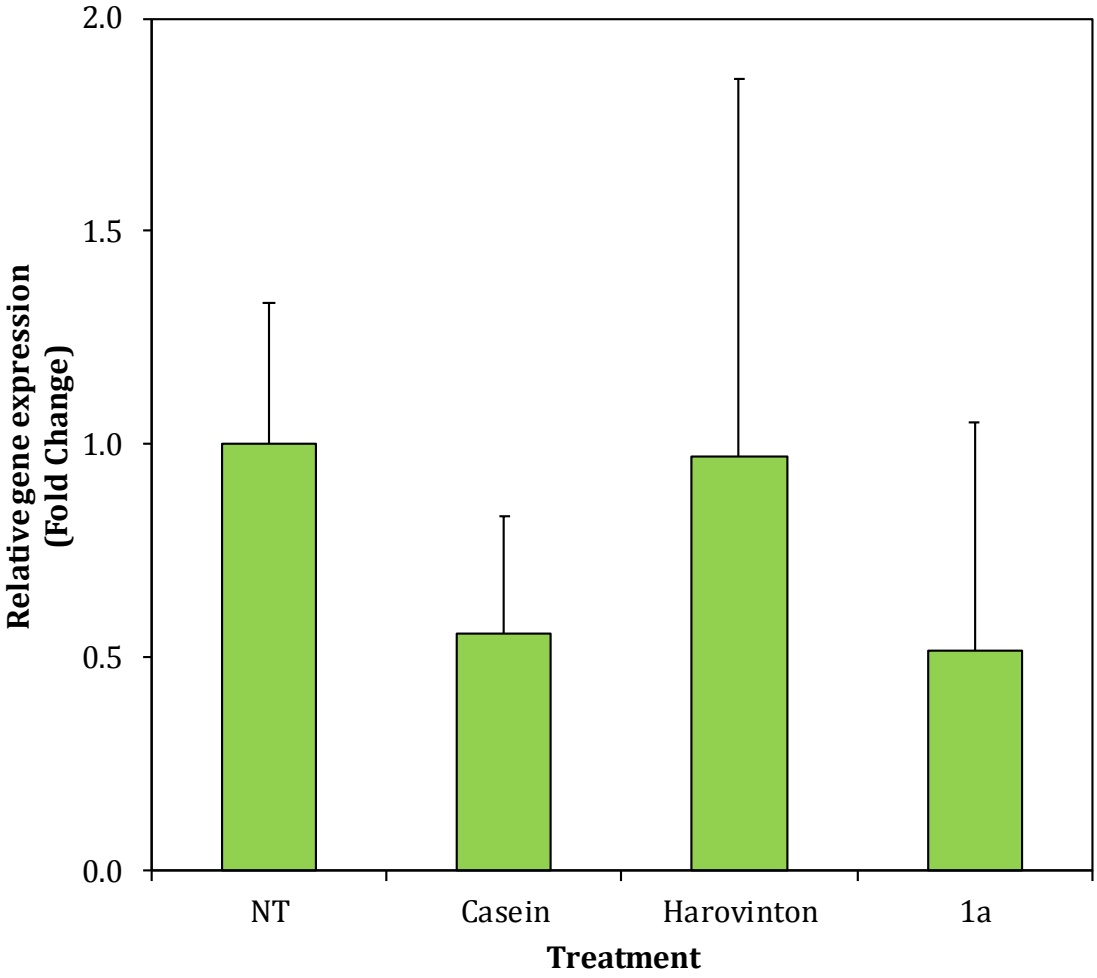


**Figure 3.11.** Gene expression levels of peroxisome proliferator- activated receptor γ *(pparγ)* in mouse 3T3-L1 cells treated with protein hydrolysates (200µg/well). Concentrations of *pparγ* mRNA were determined using Digital drop PCR. Values are mean fold differences compared to the No Treatment group ± SD (baseline=1; n=6). No significant differences were observed using one-way ANOVA analysis ($p > 0.05$) .

## 3.3 Soy-dependent changes in protein expression of PPARγ and UCP-1

To complement the RNA expression changes discussed in Section 3.1, protein levels of PPARγ and UCP-1 were also analyzed. *In vivo* rat adipose tissue samples and *in vitro* mouse 3T3-L1 samples were tested using Western blotting techniques. Protein levels of PPARγ and UCP-1 was normalized against β actin protein levels. The casein and isoflavone diet was set as the control (baseline = 1) in order to calculate fold difference.

### 3.3.1 *In vivo* experiment

Western blot analysis of both male and female rat adipose tissue revealed no significant differences in PPARγ protein expression when comparing the different treatments. Doublets were observed on the female Western blots; however the bottom band was considered as background and was not considered for densitometry analysis. The results for the male and female rats were therefore combined to observe overall expression changes. PPARγ protein levels were normalized using the corresponding β-actin band intensity measurements. Fold differences were calculated using the casein and isoflavone diet group as the control (baseline set to 1).

Although not significant, there was a small decrease in PPARγ protein levels in the in the casein diet group relative to the control (

**Figure 3.12**). The three soy diet groups, however, did show a significant increase in PPARγ protein levels in comparison to the casein diet group ($p<0.002$).

PPARγ protein levels appeared to increase slightly in rats fed soy- supplemented diets relative to the control. Rats fed 1a hydrolysates exhibited slightly higher levels of PPARγ protein than the control and SPI diet groups ($p<0.02$), while rats fed Harovinton hydrolysates showed the highest PPARγ protein levels in comparison to rats fed either SPI or 1a hydrolysates as well as in comparison to the control ($p<0.001$).

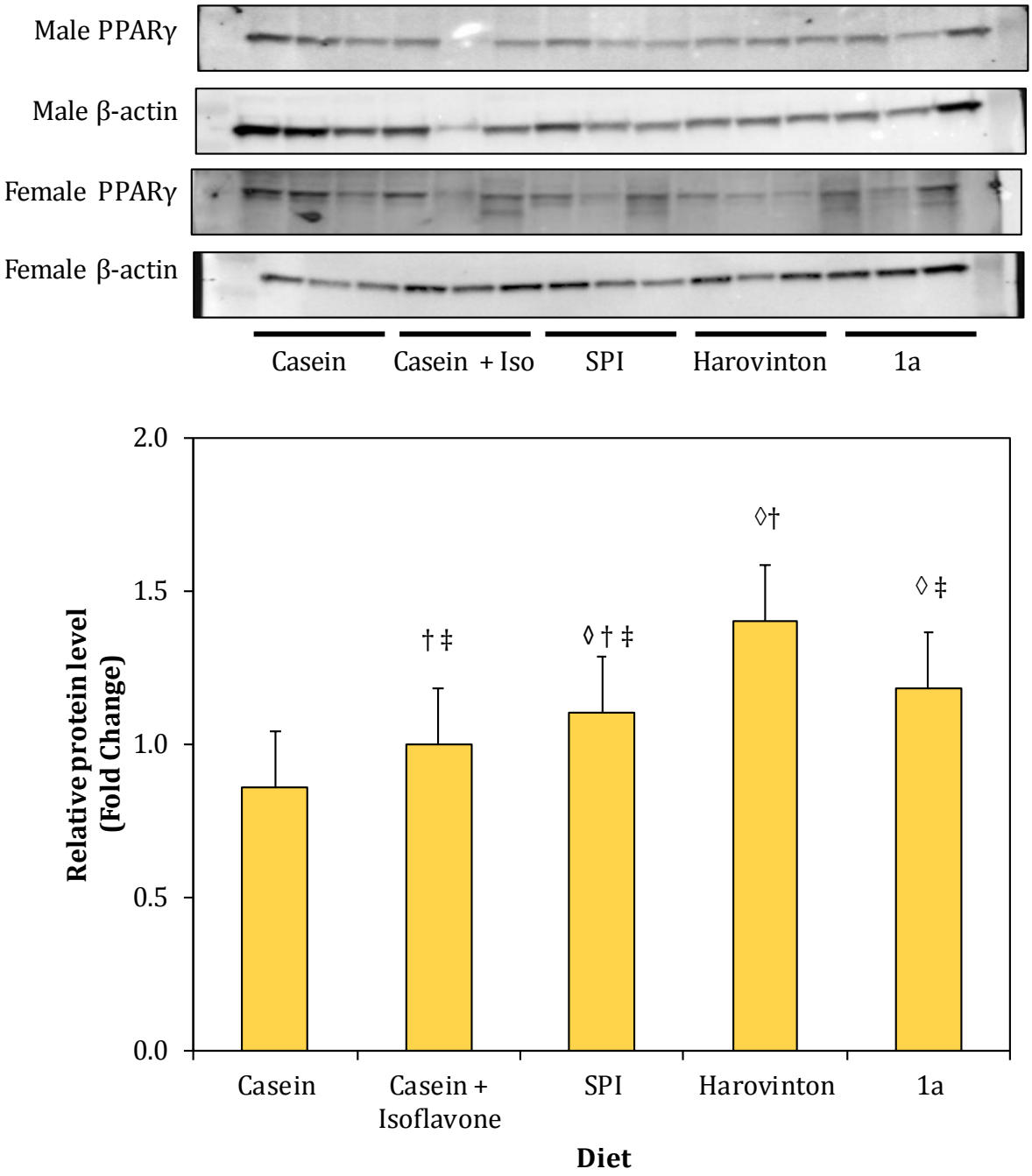


**Figure 3.12. Protein abundance of adipose peroxisome proliferator- activated receptor γ (PPARγ) in rats fed diets containing 20% protein.** Band volumes were measured using the Chemidoc Imaging System (Biorad) and normalized against β-actin band volumes. Values are mean fold differences compared to the Casein and Isoflavone group ± SD (baseline=1; male=6, female=6). Statistical significance was determined using one-way ANOVA analysis: ◊ *p≤0.002 versus Casein, † p<0.02 versus 1a, and ‡ p<0.001 versus Harovinton.*

Western blot analysis was also performed to assess protein levels of UCP-1. Most notably, UCP-1 protein levels were very variable and could not always be detected by Western blot in the male samples (Figure 3.13). Consequently, fold differences were not calculated for these samples.

The female rat samples produced much more consistent results (Figure 3.13). Similar to the trend observed in PPARγ, a decrease in UCP-1 expression in female rats fed casein was observed in comparison to the control, suggesting a possible isoflavone effect; however these differences were not significant. UCP-1 fold difference appeared higher in rats fed the control and Harovinton diet than rats fed the SPI and 1a diets.

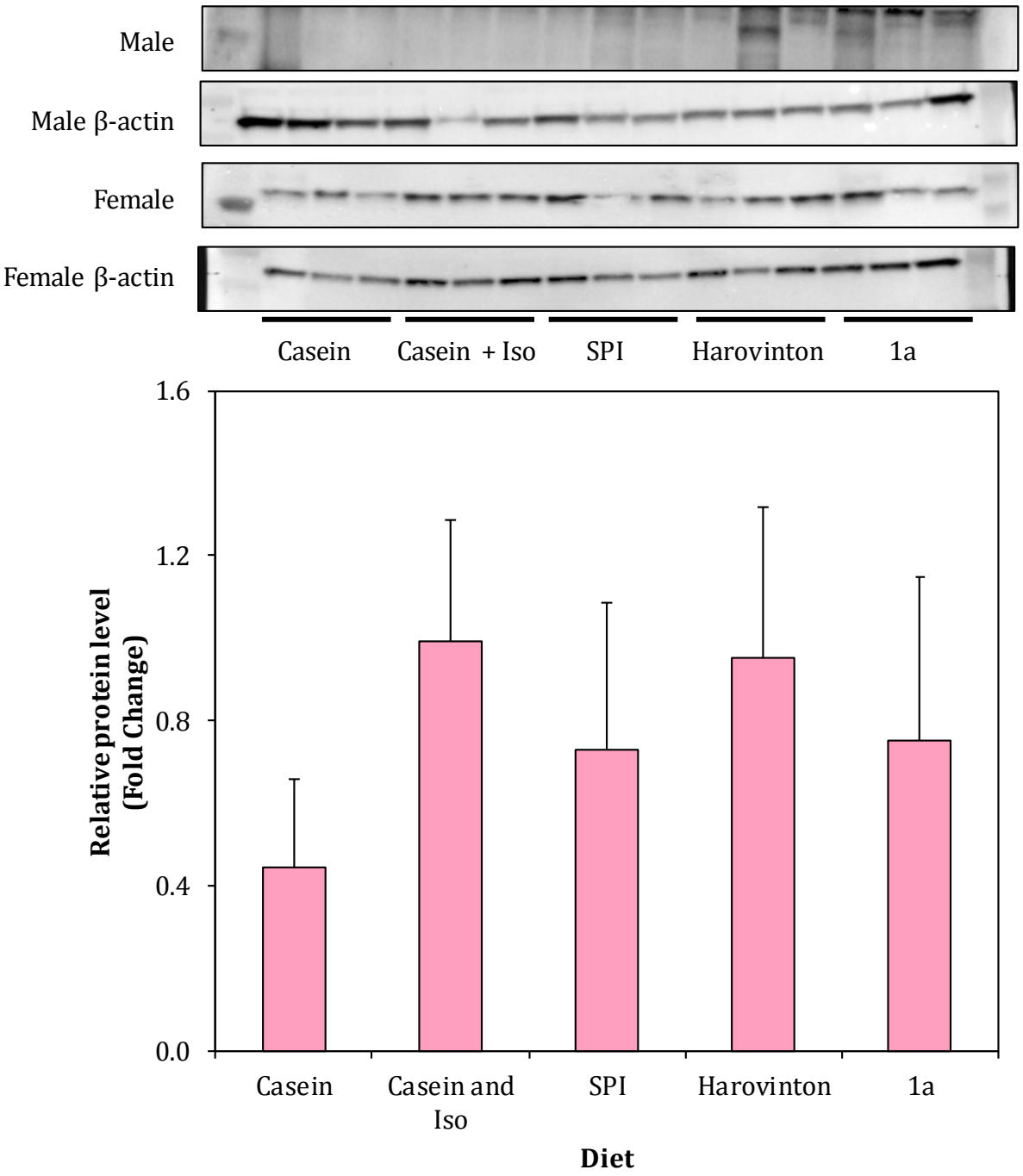


**Figure 3.13.** Protein abundance of adipose uncoupling protein-1 (UCP-1) in female rats fed diets containing 20% protein. Band volumes were measured using the Chemidoc Imaging System (Biorad) and normalized against β-actin band volumes. Values are mean fold differences compared to the Casein and Isoflavone group ± SD (baseline=1; n=6). No statistical differences were determined between diets using one-way ANOVA analysis ($p>0.05$).

### 3.3.2 *In vitro* experiment

PPARγ2 was clearly identified upon Western blotting analysis; therefore, fold differences of protein levels were determined using the No Treatment condition as the control (Figure 3.14). PPARγ1 was identified on the blot; however, because of its limited physiological significance in adipogenesis and lipid accumulation in adipose tissue, it was not studied in further detail. One-way ANOVA testing indicated an overall significance; however, secondary analysis using the Fisher LSD method did not reveal any noteworthy pairwise comparisons.

Similar overall trends were noted for total PPARγ, PPARγ1, and PPARγ2 protein levels in comparison to the control. The rosiglitazone and soy treatments appeared to decrease PPARγ protein levels, with the rosiglitazone treatment having the lowest PPARγ levels. The casein treatment seemed to reduce PPARγ protein levels more than either soy treatment.

Protein bands were not clearly or consistently obtained when testing for UCP-1 using Western blotting techniques; therefore, the results were not analyzed and no conclusions were drawn regarding UCP-1 protein levels (Figure 3.16).

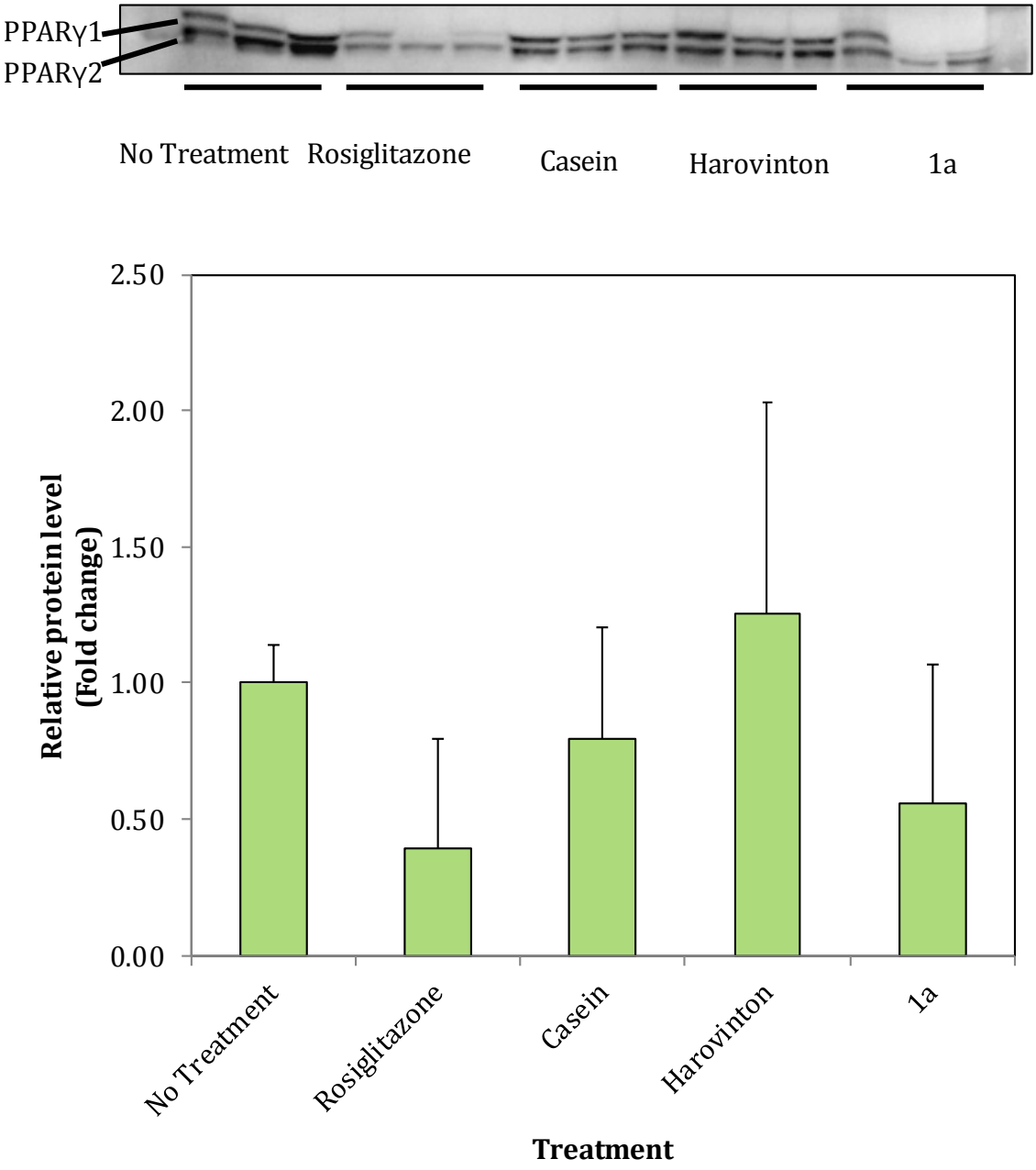


**Figure 3.14.** Protein abundance of peroxisome proliferator- activated receptor γ 2 (PPARγ2) in mouse 3T3-L1 cells treated with protein hydrolysates (200µg/well). Band volumes were measured using the Chemidoc Imaging System (Biorad) and normalized against β-actin band volumes. Values are mean fold differences compared to the No Treatment group ± SD (baseline=1; n=6). No statistically significant differences were identified one-way ANOVA analysis ($p>0.05$).

# 4 CHAPTER: DISCUSSION

Soy protein, particularly the storage proteins glycinin and β-conglycinin, are currently under investigation for their effect on lipid metabolism. As a key regulator in lipid storage, PPARγ was considered as a potential target for soy protein. Previous studies have observed lipid lowering effects of soy protein in liver and skeletal muscle through the PPARγ pathway (Yamazaki et al., 2012; Zhou et al., 2014). It was decided to expand on past research and consider the effect of soy protein on another body tissue. Due to its primary role as a lipid storage site in the body, adipose tissue was chosen as the focus of this study. Previously, soy β-conglycinin had been shown to up-regulate adipose PPARγ and prompt adipogenesis *in vitro* (Goto et al., 2013). It was therefore hypothesized that soy-mediated PPARγ expression and adipogenesis would respond similarly in a repeated *in vitro* experiment using soy strains with varying compositions of glycinin and β-conglycinin subunits. Moreover, it was hypothesized that PPARγ will be up-regulated in response to these same soy strains *in vivo*.

The Xiao lab fed Sprague-Dawley rats a high-fat diet containing soy protein concentrates from knock-out soy strains. The study revealed a significant reduction in abdominal fat in females fed soy-supplemented diets (Chen et al., 2014). The present study provided detailed results on soy-related morphological changes to WAT in an attempt to identify the mechanism by which soy protein may affect adipogenesis and lipid storage in adipose tissue, and to identify the specific soy storage protein subunit that may be involved in the proposed mechanism.

To address these hypotheses, protein and RNA were extracted from rat adipose tissue and PPARγ expression was tested by Western blot and ddPCR analysis. The results revealed UCP-1 as a second potential target of soy protein and was thus included in further protein and RNA analysis. Sex-related differences were noted in both PPARγ and UCP-1 mRNA expression and protein levels, with the females samples showing a greater response to soy consumption than their male counterparts. Noteworthy discussions on these differences are found in Section 4.2.1 and 4.3.2.

Similar testing was performed on protein and RNA extracts from 3T3-L1 cells treated with protein extracts from the knock-out soy strains. Additionally, adipogenesis efficacy in the presence of soy protein was tested in 3T3-L1 cells through visual observation and a lipid extraction assay.

## 4.1 Morphological changes in differentiated 3T3-L1 cells

Adipogenesis is the process by which immature preadipocytes undergo biochemical and morphological re-arrangement in order to become mature lipid-storing and adipokine-secreting cells. Upon differentiation, preadipocytes change from a flat elongated appearance to a rounded morphology with distinct lipid vacuoles taking up a significant part of the cytosol (Ali et al., 2013). Mouse 3T3-L1 cells were stimulated to differentiate in the presence of soy protein, and the efficacy of adipogenesis was measured by the visual assessment of differentiated morphology and by the total lipid content in the differentiated cultures.

Mouse 3T3-L1 cells are embryonic fibroblast cells that frequently serve as *in vitro* model for adipocytes (Ali et al., 2013). Differentiation is prompted by a chemical cocktail that mimics *in vivo* signalling and by high cell confluence. The control for all *in vitro* experiments relied on these two conditions to identify baseline differentiation. In this report, rosiglitazone served as the positive control for certain experiments. Rosiglitazone is a synthetic ligand that binds PPARγ and increases adipogenic activity in 3T3-L1 models (Albrektsen, Frederiksen, Holmes, Boel, Taylor, & Fleckner, 2002).

Prior to *in vitro* studies, the optimal concentrations for rosiglitazone and protein treatments were determined using concentration gradients. The optimal concentrations were determined as being those that exhibited the highest percentage of differentiation with the smallest amount of cell death manifested as cell sloughing. The chosen concentrations, 6μM rosiglitazone and 200μg/mL protein hydrosylate, were used for all subsequent *in vitro* experiments. Importantly, 200μg/mL translated into 0.0.2% w/v protein treatment, different to the 20% protein composition of the animal diets.

Additionally, casein was used as a treatment condition in all the experiments in this report. Casein is the most abundant protein in dairy products and is frequently used as a model for animal protein in nutrition studies due to its availability and cost effectiveness. Dietary animal protein has sometimes been associated with increased weight gain, thus causing popular opinion to waiver between the inclusion or exclusion of meat and dairy products in weight loss

programs (Bujnowski, Xun, Daviglus, Van Horn, He, & Stamler, 2011). Consequently, soy protein is often considered as an alternative to animal protein in the food industry as well as in weight- loss supplements. This study treated 3T3-L1 cells and rats with both casein and soy protein. This was done in order to observe whether adipose tissue responded differently in the presence of animal- or plant-based proteins.

### 4.1.1 Glycinin/β-conglycinin α' knockout strain prompts large lipid droplet formation

The complete reorganization of gene transcription required for adipogenesis is not an instantaneous process. The first wave of adipogenic genes is activated with a few hours of being exposed to differentiation stimuli, such as insulin, cAMP, and glucocorticoids, but the second wave of adipogenic genes is not activated until 24 to 48 hours later (Siersbaek et al., 2011). Consequently, rosiglitazone and protein hydrolysates were administered at the time of differentiation as well as 48 hours later in order to determine whether treatment administration time alters differentiation. Visual observation of lipid accumulation revealed similar trends for both treatment time points (Figures 3.3 & 3.4). This suggested that any effect of soy on differentiation may not be dependent on time of treatment administration. Droplet size distribution analysis also showed very similar trends in between the two treatment time points; however, statistically significant differences were only

noted when cells were treated at the time of differentiation (Figures 3.5 & 3.6). Based on these results, all subsequent *in vitro* experiments administered soy hydrolysates at the time of differentiation.

For both treatment time points, differentiation appeared to be around 80%, for all treatment conditions, but differences between treatment groups were noted when considering lipid droplet size. *In vivo,* mature WAT adipocytes are characterized by a single lipid droplet that dominates the cytosol; however, immortalized cell lines, such as mouse 3T3-L1, accumulate triglycerides in multiple smaller droplets upon differentiation (Leff et al., 2003). This typical *in vitro* morphology was observed in this experiment. For all treatments and treatment time points, the general profile showed an inverse relationship between droplet size and number of lipid droplets, with the exception of the largest droplet size group (Figures 3.5 & 3.6).

Rosiglitazone-treated cells preferentially stored lipids in much smaller droplets within the cells compared to untreated cells (Figures 3.3A &B and 3.4A&B). This was further confirmed when the size distribution of the lipid droplets was calculated. Almost 90% of all droplets in rosiglitazone-treated cells fell within the smallest size category, and there were no droplets with areas larger than $0.05mm^2$ (Figures 3.5 & 3.6). Casein and Harovinton hydrolysates prompted the formation of slightly larger lipids in comparison to rosiglitazone- treated cells (Figures 3.3C&D and 3.4C&D). Moreover, when treated at the time of differentiation, they presented very similar lipid accumulation profiles, with the only exception being a higher

percentage of droplets ranging between 0.005 and 0.01mm$^2$ observed in the Harovinton-treated cells relative to the casein-treated cells (Figure 3.5). Cells treated with the knocked-out soy strain (1a) protein hydrolysates presented the most unique lipid droplet profile, with very large lipid droplets evident within the cytosol (Figures 3.3E &3.4E). Droplet size distribution analysis revealed that while lipids were mostly stored in smaller droplets, there were significantly more medium and large droplets in this treatment group compared to the other groups when protein hydrolysates were administered at the time of differentiation (Figure 3.5). At first glance, it appeared that soy protein devoid of β-congycinin α', and glycinin might increase lipid accumulation; however, a quantitative assessment of the intracellular lipids for all protein-treated 3T3-L1 cells was required in order confirm this speculation.

### 4.1.2 Glycinin and β-conglycinin α' may not be involved in changes in lipid accumulation

Quantification of the extracted Oil Red O from protein-treated 3T3-L1 cells revealed less dramatic differences in lipid accumulation than the microscopic observations. The rosiglitazone treatment prompted a significant increase in lipid accumulation in relation to the untreated cells and the cells treated with either casein or Harovinton hydrolysates (Figure 3.7). Treatment with casein decreased lipid accumulation, and there was a small increase in lipid accumulation in cells treated with soy protein hydrolysates relative to the untreated cells.

The observed soy-mediated increase in lipid accumulation corresponded with a similar study performed by Goto et al. (2013). They measured relative lipid accumulation in 3T3-L1 cells treated with different concentrations of commercial soy protein hydrolysates. They reported a 1.2- and 1.3- fold increase in lipid accumulation with the administration of 100μg/mL and 300μg/mL of soy protein, respectively. My results for a 200μg/mL treatment showed a 1.1-fold increase in lipid accumulation.

A slight increase in lipid accumulation was observed when cells were treated with 1a hydrolysates relative to cells treated with Harovinton hydrolysates. Although the difference was not statistically significant, the similar lipid accumulation levels suggest that β-conglycinin's α' subunit and glycinin may not be involved in improving lipid loading in adipocytes. Any increase in lipid accumulation observed in the soy protein-treated cells relative to the control or casein-treated cells may be accounted to the activity of a yet undetermined soy peptide.

## 4.2 Changes in mRNA expression

The differentiation process that converts preadipocytes into mature, lipid-storing adipocytes involves the complex activation and inactivation of promoter and inhibitor genes (Siersbaek et al., 2012). The hypothesis of this study was that PPARγ, being the key adipogenic regulator, would show some soy-dependent

changes in expression; however, I also analyzed the samples for note-worthy mRNA expression changes in any other genes that are involved in adipogenesis and lipid accumulation in white and brown adipose tissue.

The expression of 84 genes involved in adipogenesis and the maintenance of mature adipocyte function was assessed using rat mRNA. The rat diets, unlike the protein treatments administered to the 3T3-L1 cells, contained isoflavones. The casein and isoflavone diet group was thus used as the control in order to simultaneously observe differences in expression between the animal- and soy protein diet groups.

No change in *pparγ* mRNA expression was observed in any of the diets. The only gene that showed changes in expression was *ucp-1.* This gene appeared to be expressed at higher levels in WAT of male rats fed SPI and Harovinton (Figure 3.8 B &C). No change in *ucp-1* mRNA expression was observed in rats fed casein or 1a hydrolysates (Figure 3.8 A &D). These results indicated that isoflavones are not involved in the observed *ucp-1* expression changes. Moreover, it appeared that β-conglycinin α' and glycinin may be involved in altering *ucp-1* expression.

### 4.2.1 Glycinin/β-conglycinin α' affects *pparγ* expression in a sex-dependent manner

Although no expression change was observed in the adipogenesis array, *pparγ* gene expression was still analyzed in more detail using Digital Drop PCR (ddPCR). Peroxisome-proliferator activated receptor γ is the key regulator of adipogenesis.

Activated by genes from early adipogenesis, PPARγ prompts a cascade of genetic transcription that results in the restructuring of preadipocytes into mature adipocytes (Rosen and Spiegelman, 2000). Without this transcription factor, adipogenesis is unable to proceed (Rosen et al., 1999). Due to its crucial role in adipogenesis, soy-related changes in *pparγ* expression remained as a primary focus in this report.

The initial qPCR analysis was performed on male samples only; therefore expression of *pparγ* was further analyzed in male and female mRNA using ddPCR. As expected, there was very little change in *pparγ* gene expression between the male diet groups (Figure 3.9). The Harovinton and 1a diet group showed a slight decrease in expression of the target gene relative to the casein and isoflavone diet, initially suggesting that soy protein may not be involved in *pparγ* gene expression changes. Contrary to this data, a slight decrease in *pparγ* gene expression in the casein diet group in relation to the SPI diet group was observed. The results from these two isoflavone-free diet groups suggested that soy protein may be involved in up-regulating *pparγ* expression relative to casein. Thus no conclusion was able to be drawn regarding the impact of soy protein on *pparγ* expression levels. Interestingly, the casein diet group showed lower expression levels in the target gene relative to the casein and isoflavone, Harovinton, and 1a diet groups. This suggested that *pparγ* gene expression in male rats may be affected by soy isoflavones.

Female rats exhibited very different *pparγ* gene expression levels than their male counterparts. Overall, *pparγ* gene expression levels were much higher in the female rats than in the male rats. There was an observed increase in *pparγ* gene expression in the Harovinton diet group relative to the casein and isoflavone diet group and an increase in expression in the SPI diet group relative to the casein group. Both these observations indicated that soy protein may indeed be involved in the up-regulated expression of the target gene. Moreover, the casein diet group showed higher *pparγ* gene expression levels than the casein and isoflavone diet group, but lower expression levels than the Harovinton group. This indicated that isoflavones may not alter *pparγ* gene expression in female rats. Female rats fed 1a protein exhibited much lower expression levels of the target gene than female rats fed Harovinton protein. This suggested that β-conglycinin α' subunit or glycinin may be involved in regulating *pparγ* gene expression in female rats.

Sex-related differences were also observed in the initial study from which this project developed. Chen et al. (2014) observed a decrease in abdominal fat in female rats fed soy protein relative to their male counterparts. This observation coupled with the results from the present study may suggest a method of weight management for soy protein. In obesity, pro-inflammatory signals released by WAT macrophages inhibit *pparγ* expression and insulin sensitivity and prompt apoptosis in adipocytes (Ali et al., 2013). The overall result of these responses is ectopic fat deposits. Moreover, abdominal fat, particularly visceral abdominal fat, typically favours hypertrophy instead of cell proliferation in order to accommodate more

lipids, a potentially harmful practice since larger adipocytes are less responsive to insulin (White & Tchoukalova, 2013; Yang et al., 2012). The results from the present study indicate an increase in *pparγ* gene expression in female abdominal WAT in response to Harovinton hydrolysates. This increased expression may help counter the effects of obesity-induced pro-inflammatory signals by prompting preadipocyte differentiation instead of adipocyte hypertrophy, thereby maintaining insulin responsiveness and preventing ectopic fat deposition. Further research would be required in order to confirm these theories.

In order to support the *in vivo* results and ensure that isoflavones were not involved in the observed results, 3T3-L1 cells were treated with isoflavone-free protein hydrolysates. The results from this study support the results from the female rat ddPCR analysis. Cells treated with Harovinton hydrolysates exhibited much higher *pparγ* gene expression levels relative to cells treated with casein hydrolysates (Figure 3.11). This result supported the conclusion that soy protein may indeed affect *pparγ* gene expression. Additionally, cells treated with 1a hydrolysates showed decreased expression of the target gene relative to cells treated with Harovinton. Once again, this result supported the conclusion drawn from the female rat experiment that suggested that β-conglycinin α' subunit or glycinin may indeed be involved in regulating *pparγ* gene expression.

### 4.2.2 Glycinin/β-conglycinin α' decreases *ucp-1* gene expression

Uncoupling protein-1 presented an interesting expression profile in the adipogenesis array and was therefore analyzed more carefully in the samples. Primarily found in BAT, UCP-1 diffuses the electrochemical gradient the electron transport chain in order to convert the chemical potential into heat. This decreases the metabolically available energy obtained from food sources while increases body temperature (Canon & Nedergaard, 2004). This is the rationale behind the scientific interest in BAT as a weight management tool; research is currently pursuing the possibility of converting WAT into BAT (Asano et al., 2013). Consequently, the changes in *ucp-1* gene expression in the adipogenesis array were noted with interest and further analysis was conducted in this study.

Unlike *pparγ,* no sex-related differences were observed in *ucp-1* gene expression (Figure 3.10). An isoflavone effect was noted when comparing gene expression in the casein diet group with the casein and isoflavone diet group; however, the Harovinton diet groups only revealed a slight elevation in *ucp-1* gene expression levels relative to the SPI and casein diet group. This suggested that the isoflavone effect may not significantly affect the results from this experiment.

Rats fed the SPI diet showed a small increase in *ucp-1* expression relative to rats fed the casein diet, although these results were not significant. Harovinton hydrolysates appeared to inhibit *ucp-1* gene expression in rats relative to rats fed casein and isoflavones or 1a hydrolysates. Similar expression levels were observed

between the casein and isoflavone and 1a diet groups. These results suggest that β-conglycinin α' and glycinin may be involved in inhibiting ucp-1 gene expression in rats, evidenced by the low expression levels observed in the Harovinton diet group relative to the 1a diet group.

## 4.3 Changes in protein levels

While expression of mRNA is often used to predict protein abundance, it is not always an accurate representation of actual protein levels within the cell. As a result, protein abundance of PPARγ and UCP-1 was analyzed in order to complement the mRNA results. Relative protein abundance was considered for each diet group; however these results did not provide PPARγ and UCP-1 concentrations in each sample. A standard curve should have been used to assess the validity of the densitometry analysis and to provide more quantitative results.

### 4.3.1 Glycinin/β-conglycinin α' increases PPARγ protein levels

The results from the protein analysis supported the conclusions drawn from the mRNA analysis of *pparγ* gene expression. The only difference between the two assays was that no sex-related differences were observed when considering PPARγ protein levels.

Initially, isoflavones appeared to play a role in PPARγ protein levels. The rats fed diets containing isoflavones had notably higher levels of the target protein than

the rats fed the analogous isoflavone-free diets (Figure 3.12). *In vitro* analysis using soy protein devoid of isoflavones confirmed that soy does indeed affect PPARγ protein levels; therefore, it was decided that the presence of isoflavones did not alter the conclusions drawn from this study (Figure 3.14).

For both the *in vivo* and *in vitro* experiments, soy protein treatments corresponded with higher PPARγ protein levels. *In vivo,* PPARγ protein levels were significantly increased in rats fed SPI relative to rats fed casein (Figure 3.12). Moreover, rats fed either Harovinton or 1a diets exhibited higher levels of the target protein relative to rats fed casein and isoflavones. These results confirmed literature results that soy protein does increase cellular PPARγ protein levels (Goto et al., 2013).

The results indicated that β-conglycinin α' and glycinin were involved in the observed increase in PPARγ. Rats fed the 1a diet group exhibited significantly less PPARγ protein than rats fed the Harovinton diet. These results were confirmed through *in vitro* analysis. Further experimentation will be required to determine the specific subunit that may be responsible for these results.

### 4.3.2 Glycinin/β-conglycinin α' may not affect UCP-1 protein levels in females

The role of soy proteins in mediating UCP-1 protein levels was not clear at the end of this study. Normally, UCP-1 is not expressed in WAT; by definition, any adipose tissue expressing UCP-1 is considered as BAT (Canon & Nedergaard, 2004).

Consequently, the results for UCP-1 protein levels, as well as the results from the mRNA analysis, were reflective of the amount of brown adipose tissue present in the rat abdomens. Brown fat is often found surrounding vital organs in rodents or interspersed among WAT, which may explain why it may have been collected with the abdominal WAT samples in this study (Canon & Nedergaard, 2004). Nonetheless, protein analysis of UCP-1 was still a topic of interest in this study. Previous studies have found that diet can prompt WAT to begin expressing UCP-1, thus increasing the population of thermogenic adipose tissue in order to reduce weight gain (Asano et al., 2013). Therefore, I analyzed UCP-1 protein levels in order to determine whether soy protein altered UCP-1 expression levels in WAT.

Protein levels of UCP-1 were highly variable between the sexes. Male rats did not exhibit consistent UCP-1 levels between the diets; therefore, protein analysis was unable to be performed (Figure 3.13). Female rats, however, presented a much more consistent UCP-1 protein profile between the diet groups. Similar to the mRNA results, SPI increased UCP-1 levels relative to casein, indicating that soy protein may indeed affect target protein levels. A slight isoflavone effect was noted, evidenced by the higher UCP-1 protein levels in the three isoflavone diets (Figure 3.14). Further analysis of these three diet groups revealed that β-conglycinin α' and glycinin did not affect UCP-1 protein levels. The absence of β-conglycinin α' and glycinin appeared to decrease UCP-1 expression. Overall, the results were not consistent and firm conclusion was not able to be drawn regarding the involvement of soy protein in UCP-1 protein levels.

*In vitro* analysis of UCP-1 protein levels was considered in order to determine whether soy protein was able to prompt UCP-1 expression in WAT. UCP-1 was inconsistently expressed among the treatment groups; therefore, while no conclusion could be drawn, it was speculated that soy protein may not be involved in converting WAT to BAT. Further experiments are required in order to determine whether soy protein is able to increase non-shivering thermogenesis in mammals.

## 4.4 Conclusions and future directions

Using *in vitro* analysis, this report showed that soy protein increased lipid accumulation in adipocytes. Soy protein increased lipid droplet size and slightly increased cellular lipid levels. Specifically, the glycinin/β-conglycinin α' knockout strain prompted the greatest increase in lipid droplet size and lipid accumulation relative to the other soy treatments. This indicated that an unknown soy protein may be involved in altering lipid accumulation in adipose tissue.

Both *in vitro* and *in vivo* analysis revealed that soy protein affects adipogenesis through PPARγ in a sex-dependent manner. Soy protein affected gene expression and protein levels preferentially in females than males. This report revealed that soy protein increased *pparγ* gene expression and PPARγ protein levels in 3T3-L1 cells and in female rat adipose tissue. Moreover, it was shown that glycinin and β-conglycinin α' were involved in the observed increases in gene expression (Figure 3.9, $p<0.03$) and protein levels of PPARγ (Figure 3.12, $p<0.001$). A functional assay

should be performed in the future to further understand the interaction between soy peptides and PPARγ.

This report was unable to draw firm conclusions regarding the effect of soy protein on converting WAT to BAT. *In vivo* analysis revealed that soy protein affected *ucp-1* gene expression. Specifically, the glycinin/β-conglycinin α' storage proteins decreased *ucp-1* gene expression but did not appear to affect UCP-1 protein levels. Overall, it was suggested that soy protein was not involved in converting WAT to BAT. Increasing the sample size in both the mRNA and protein experiments would provide more statistical significance to this study.

While soy protein may not be a candidate for stimulating non-shivering thermogenesis in mammals, it is still a valuable asset in terms of weight management. Based on this report, soy storage proteins are involved in maintaining healthy adipose tissue functioning. As a continuation to this project, focus could be given to identifying the bioactive soy glycinin or β-conglycinin subunit(s) associated with PPARγ expression. One possible approach would be to measure PPARγ mRNA and protein levels in adipose tissue from rats fed different glycinin/β-conglycinin knock-out strains. Such strains have already been developed by Agriculture and Agri-Food Canada (Zarkadas et al., 2006). Determining the bioactive soy peptide(s) could be valuable for the future development of an anti-obesity strain of soybeans for commercial production.

**REFERENCES**


Albrektsen, T., Frederiksen, K., Holmes, W., Boel, E., Taylor, K., & Fleckner, J. (2002). Novel Genes Regulated by the Insulin Sensitizer Rosiglitazone During Adipocyte Differentiation. *Diabetes*. 51 (4), 1042-1051.

Alezandro, M. R., Granato, D., Lajolo, F. M., & Genovese, M. I. (2011). Nutritional aspects of second generation soy foods. *J Agri Food Chem*. 59(10), 5490-97.

Ali, A. T., Hochfeld, W. E., Myburgh, R., & Pepper, M. S. (2013). Adipocyte and adipogenesis. *Eur J Cell Biol.* 92(6-7), 229-36.

Amigo-Benavent, M., Athanasopoulos, V.I., Ferranti, P., Villamiel, M., & del Castillo, M.D. (2009). Carbohydrate moieties on the in vitro immunoreactivity of soy β-conglycinin. *Food Res Intl*. 42 (7), 819-825.

Arkan, M.C., Hevener, A.L., Greten, F.R., Maeda, S., Li, Z.W., Long, Wynshaw-Boris, A., Poli, G., Olefsky, J., & Karin, M. (2005). IKK-β links inflammation to obesity-induced insulin resistance. *Nat. Med.* 11,191–98

Asano, H., Yamada, T. F., Hashimoto, O. F., Umemoto, T. F., Sato, R. F., Ohwatari, S. F., et al. (2013). Diet-induced changes in Ucp1 expression in bovine adipose tissues. *Gen Comp Endocrinol*. 184 (Apr), 87-92.

Baba, N. H., Sawaya, S. F., Torbay, N. F., Habbal, Z. F., Azar S FAU - Hashim,,S.A., & Hashim, S. A. (1999). High protein vs high carbohydrate hypoenergetic diet for the treatment of obese hyperinsulinemic subjects. *Int J Obes Relat Metab Disord*. 23(11), 1202-6.

Beilson, V., Chen, Z., Shoemaker, C., Fischer, L., Goldberg, B., & Neilson, C. (2002). Genomic organization of glycinin genes in soybean. *Theor Appl Genet*. 104(6-7), 1132-40.

Bujnowski, D., Xun, P., Daviglus, M.L., Van Horn, L., He, K., & Stamler, J. (2011). Longitudinal association between animal and vegetable protein intake and obesity among men in the United States: the Chicago Western Electric Study. *J Am Diet Assoc*. 111(8):1150-1155.

Buzzell, R. I., Anderson, T. R., Hamill, A. S. & Welacky, T. W. (1991). Harovinton soybean. *J. Plant Sci.* 71: 525-526

Cannon, B., & Nedergaard, J. (2004). Brown adipose tissue: Function and physiological significance. *Physiol Rev*. 84(1), 277-359.

Chen, Q., Wood, C., Gagnon, C., Cober, E., Frégeau-Reid, J., Gleddie, S., & Xiao, C. (2014). The α' subunit of β-conglycinin and the A1-5 subunits of glycinin are not essential for many hypolipidemic actions of dietary soy proteins in rats. *Eur J of Nutrition*. 53(5), 1195-207.

Choi, S.S., Cha, B.Y., Lee, Y.S., Yonezawa, T. F., Teruya, T., Nagai, K., & Woo, J.T. (2009). Magnolol enhances adipocyte differentiation and glucose uptake in 3T3-L1 cells. *Life Sci*. 84(25-26), 908-14.

Choi, S., Adachi, M., & Utsumi, S. (2002). Identification of the bile acid-binding region in the soy glycinin A1aB1b subunit. *Biosci, Biotechnol, and Biochem.* 66(11), 2395-2401.

Christodoulides, C., Lagathu, C., Sethi, J. K., & Vidal-Puig, A. (2009). Adipogenesis and WNT signalling. *Trends Endocrinol Metab*. 20(1), 16–24.

Coates, J. B., Medeiros, J. S., Thanh, V. H., & Nielsen, N. C. (1985). Characterization of the subunits of β-conglycinin. *Arch Biochem Biophys*. 243(1), 184-194.

Coppack, S. W. (2001). Pro-inflammatory cytokines and adipose tissue. *Proc Nutr Soc.* 60(3), 349-56.

Cornelius, P., MacDougald, O. A., & Lane, M. D. (1994). Regulation of adipocyte development. *Annu Rev Nutr*. 14(1), 99-129.

Deeb, S. S., Fajas, L., Nemoto, M., Pihlajamaki, J., Mykkanen, L., Kuusisto, J., Laakso, M., Fujimoto, W., Auwerx, J. (1998). A pro12ala substitution in PPAR-gamma-2 associated with decreased receptor activity, lower body mass index and improved insulin sensitivity. *Nature Genet*. 20: 284-287.

Desvergne, B., & Wahli, W. (1999). Peroxisome proliferator-activated receptors: Nuclear control of metabolism. *Endocr Rev.* 20(5), 649-88.

Feingold, K.R., Grunfeld, C. 1987. Tumor necrosis factor-α stimulates hepatic lipogenesis in the rat in vivo. *J. Clin. Investig.* 80:184–90.

Friedman, M., & Brandon, D. L. (2001). Nutritional and health benefits of soy proteins. *J Agri Food Chem.* 49(3), 1069-86.

Fujikura, J., Fujimoto, M., Yasue, S., Noguchi, M., Masuzaki, H., Hosoda, K., Tachibana, T., Sugihara, H., & Nakao, K. (2005). Insulin-induced lipohypertrophy: report of a case with histopathology. *Endocr J*. 52(5):623-8.

Gonzalez de Mejia, E., Martinez-Villaluenga, C., Roman, M., & Bringe, N. A. (2010). Fatty acid synthase and in vitro adipogenic response of human adipocytes inhibited by a and a' subunits of soybean ß-conglycinin hydrolysates. *Food Chem*. 119(4), 1571-77.

Gotherstrom, C., Ringden, O., Westgren, M., Tammik, C., & Le Blanc, K. (2003). Immunomodulatory effects of human foetal liver-derived mesenchymal stem cells. *Bone Marrow Transplant*. 32(3), 265-72.

Goto, T., Mori, A., & Nagaoka, S. (2013). Soluble soy protein peptic hydrolysate stimulates adipocyte differentiation in 3T3-L1 cells. *Mol Nutr Food Res.* 57(8), 1435-45.

Gregoire, F. M. (2001). Adipocyte differentiation: From fibroblast to endocrine cell. *Exp Biol Med*. 226(11), 997-1002.

Health Canada. (2015). Summary of Health Canada's Assessment of a Health Claim about Soy Protein and Cholesterol Lowering. From *Bureau of Nutritional Sciences, Food Directorate, Health Products and Food Branch*. pp.1-12.

Henkel, J. (2000). Soy. health claims for soy protein, questions about other components. *FDA Consum*. 34(4), 13-5, 18-20.

Hirosumi, J., Tuncman, G., Chang, L., Gorgun, C.Z., Uysal, K.T., Maeda, K., Karin, M., & Hotamisligil, G. (2002). A central role for JNK in obesity and insulin resistance. *Nature.* 420:333–36

Hotamisligil, G. S., & Spiegelman, B. M. (1994). Tumor necrosis factor alpha: A key component of the obesity-diabetes. *Diabetes.* 43(11), 1271-78.

Inoue, N., Fujiwara, Y., Kato, M., Funayama, A., Ogawa, N., Tachibana, N., Kohno, M., & Ikeda, I. (2015). Soybean β-conglycinin improves carbohydrate and lipid metabolism in Wistar rats. *Biosci Biotechnol Biochem*. 79(9), 1528-34.

Janssen, I. (2013). The public health burden of obesity in canada. *Can J Diabetes*. 37(2), 90-96.

Jiang, G., Li, L., Fan, J., Zhang, B., Oso, A., Xiao, C., & Yin, Y. (2015). Dietary soy isoflavones differentially regulate expression of the lipid-metabolic genes in different white adipose tissues of the female Bama mini-pigs. *Biochem and Biophys Res Commun.* 461(1), 159-64.

Kanda, H., Tateya, S., Tamori, Y., Kotani, K., Hiasa, K., Kitazawa, R., et al. (2006). MCP-1 contributes to macrophage infiltration into adipose tissue, insulin resistance, and hepatic steatosis in obesity. *J Clin Invest*. 116(6), 1494-1505.

Kang, J. W., Nam, D., Kim, K. H., Huh, J. E., & Lee, J. D. (2013). Effect of gambisan on the inhibition of adipogenesis in 3T3-L1 adipocytes. *Evid Based Complement Alternat Med.* 2013 (2013), 11 pages.

Kavurma, M. M., Bhindi, R., Lowe, H. C., Chesterman, C., & Khachigian, L. M. (2005). Vessel wall apoptosis and atherosclerotic plaque instability. *J Thromb Haemost.* 3(3), 465-472.

Khan, T., Muise, E. S., Iyengar, P., Wang, Z. V., Chandalia, M., Abate, N., et al. (2009). Metabolic dysregulation and adipose tissue fibrosis: Role of collagen VI. *Mol Cell Biol.* 29(6), 1575-1591.

Khatib, K. A., Herald, T. J., Aramouni, F. M., MacRitchie, F., & Schapaugh, W. T. (2002). Characterization and functional properties of soy β-conglycinin and glycinin of selected genotypes. *J Food Sci*, 67(8), 2923-2929.

Kirk, E. A., Sutherland P FAU - Wang,,S.A., FAU, W. S., Chait A FAU - LeBoeuf,,R.C., & LeBoeuf, R. C. (1998). Dietary isoflavones reduce plasma cholesterol and atherosclerosis in C57BL/6 mice but not LDL receptor-deficient mice. *J Nutr*. 128(6), 954-9.

Kohno, M., Hirotsuka, M., Kito, M., & Matsuzawa, Y. (2006). Decreases in serum triacylglycerol and visceral fat mediated by dietary soybean β-conglycinin. *J Atheroscler Thromb*. 13(5), 247-255.

Lagari, V. S., & Levis, S. (2013). Phytoestrogens in the prevention of postmenopausal bone loss. *J Clin Densitom*. 16(4):445–449

Lakemond, C. M. M., de Jongh, Harmen H. J., Hessing, M., Gruppen, H., & Voragen, A. G. J. (2000). Soy glycinin: influence of pH and ionic strength on solubility and molecular structure at ambient temperatures. *J Agri Food Chem*. 48(6), 1985-1990.

Larsen, T. M., Toubro, S., & Astrup, A. (2003). PPARgamma agonists in the treatment of type II diabetes: Is increased fatness commensurate with long-term efficacy? *Int J Obes (Lon).* 27(2), 147-61.

Leff, T., FAU, M. S., & Camp, H. S. (2004). Review: Peroxisome proliferator-activated receptor-gamma and its role in the development and treatment of diabetes. *Exp Diabesity Res.* 5(2), 99-109.

Lessard, J., & Tchernof, A. (2012). Depot- and obesity-related differences in adipogenesis. *J Clin Lipidol*. 7(5), 587-596.

Lin, Y., Meijer, G.W., Vermeer, M.A., & Trautwein, E.A. (2004). Soy Protein Enhances the Cholesterol-Lowering Effect of Plant Sterol Esters in Cholesterol-Fed Hamsters. *J. Nutr.* 134(1), 143-148.

Lovati, M. R., Manzoni, C. F., Canavesi, A. F., Sirtori, M. F., Vaccarino, V. F., Marchi, M. F., et al. (1987). Soybean protein diet increases low density lipoprotein receptor activity in mononuclear cells from hypercholesterolemic patients. *J Clin Invest*. 80(5), 498-502.

MacIas-Gonzalez, M., Moreno-Santos, I., GarcÃa-Almeida, J. M., Tinahones, F. J., & Garcia-Fuentes, E. (2009). PPARγ protects against obesity by means of a mechanism that mediates insulin resistance. *Eur J Clin Invest*. 39(11), 972-9.

Madsen, L., Pederson, L.M., Liaset, B., Ma, T., Petersen, R.K.,, van der Berg, S., Pan, J., Muller-Decker, K., Dulsen, E.D., Kleeman, R., Kooistra, T., Døskland, S.O., & Kristiansen, K. (2008). cAMP-dependent Signaling Regulates the Adipogenic Effect of n-6 Polyunsaturated Fatty Acids. *J Biol Chem*. 283, 7196-7205.

Marieb, E.N., & Hoehn, K. (2007). "Chapter 4: Tissue: The Living Fabric. From *Human Anatomy and Physiology.* 7 ed. pp. 132.

Marsh, T. G., Straub, R. K., Villalobos, F., & Hong, M. Y. (2011). Soy protein supports cardiovascular health by downregulating hydroxymethylglutaryl-coenzyme A reductase and sterol regulatory element-binding protein-2 and increasing antioxidant enzyme activity in rats with dextran sodium sulfateâ€"induced mild systemic inflammation. *Nutr Res*. 31(12), 922-8.

Martinez-Villaluenga, C., Dia, V. P., Berhow, M., Bringe, N. A., & Gonzalez de Mejia, E. (2009). Protein hydrolysates from ß-conglycinin enriched soybean genotypes inhibit lipid accumulation and inflammation in vitro. *Mol Nutr Food Res*. 53(8), 1007-18.

Medina-Gomez, G., Gray, S., & Vidal-Puig, A. (2007). Adipogenesis and lipotoxicity: Role of peroxisome proliferator-activated receptor γ (PPARγ) and PPARγ coactivator-1 (PGC1). *Public Health Nutr*. 10(10), 1132-37.

Michalik, L., Desvergne, B., Tan, N. S., Basu-Modak, S., Escher,P., Rieusset, J., Peters, J. M., Kaya, G., Gonzalez, F. J., Zakany, J.,Metzger, D., Chambon, P., Duboule, D., and Wahli,W. (2001) Impaired skin wound healing in peroxisome proliferator-activated receptor (PPAR)alpha and PPARbeta mutant mice. *J Cell Biol.* 154, 799–814.

Moreno-Navarrete, J.M., & Fernández-Real, J.M. (2012). Chapter 2: Adipocyte differentiation. From *Adipose Tissue Biology*. M.E. Symonds (ed.). Springer. 17-38.

Morita, T., Oh-hashi, A., Takei, K., Ikai, M., Kasaoka, S., & Kiriyama, S. (1997). Cholesterol-lowering effects of soybean, potato and rice proteins depend on their low methionine contents in rats fed a cholesterol-free purified diet. *J Nutr*. 127(3), 470-7.

Nagasawa, A., Fukui, K., Kojima, M., Kishida, K., Maeda, N., Nagaretani, H., et al. (2003). Divergent effects of soy protein diet on the expression of adipocytokines. *Biochem Biophys Res Comm*. 311(4), 909-14.

Nakachi, Y., Yagi, K., Nikaido, I., Bono, H., Tonouchi, M., Schönbach, C., & Okazaki, Y. (2008). Identification of novel PPARγ target genes by integrated analysis of ChIP-on-chip and microarray expression data during adipocyte differentiation. *Biochem Biophys Res Comm*. 372(2), 362-366.

Pal, P., Lochab, S., Kanaujiya, J. K., Kapoor, I., Sanyal, S., Behre, G., et al. (2013). E3 ubiquitin ligase E6AP negatively regulates adipogenesis by downregulating proadipogenic factor C/EBPalpha. *PLoS One*. 8(6), e65330.

Palacios-Gonzalez, B., Zarain-Herzberg, A., Flores-Galicia, I., Noriega, L. G., Aleman-Escondrillas, G., Zarinan, T., et al. (2014). Genistein stimulates fatty acid oxidation in a leptin receptor-independent manner through the JAK2-mediated phosphorylation and activation of AMPK in skeletal muscle. *Biochimica Et Biophysica Acta*. 1841(1), 132-40.

Preedy, V. R., Watson, R. R., & Patel, V. B. (2011). Section A.1. A Primer on Seed and Nut Biology, Improvement, and Use. From *Nuts and seeds in health and disease prevention*. NL: Academic Press. pp. 7-10.

Petruccelli, S., & Anon, M. C. (1995). Soy protein isolate components and their interactions. *J Agri Food Chem.* 43(7), 1762-7.

Rosen, E. D., Hsu, C.H., Wang, X., Sakai, S., Freeman, M.W., Gonzalez, F.J., & Spiegelman, B.M. (1999). C/EBPalpha induces adipogenesis through PPARgamma: a unified pathway. *Genes Dev.* 16(1):22-6.

Rosen, E. D., & Spiegelman, B. M. (2000). Molecular regulation of adipogenesis. *Annu Rev Cell Dev Biol.* 16:145-71.

Seale, P., & Lazar, M. A. (2009). Brown fat in humans: Turning up the heat on obesity. *J Diabetes*. 58(7), 1482-4.

Seo, S. G., Yang, H., Shin, S. H., Min, S., Kim, Y. A., Yu, J. G., et al. (2013). A metabolite of daidzein, 6,7,4'-trihydroxyisoflavone, suppresses adipogenesis in 3T3-L1 preadipocytes via ATP-competitive inhibition of PI3K. *Mol Nutr Food Res.* 57(8), 1446-55.

Siersbæk, R., Nielsen, R., Mandrup, S.(2012). Transcriptional networks and chromatin remodeling controlling adipogenesis. *Trends Endocrinol Metab*. 23 (2) pp: 56-64.

Soy Canada. (2014). Home page. Online. http://soycanada.ca/

Staswick, P.E., Hermodson, M.A., & Nielson, N.C. (1981). Identification of the acidic and basic subunit complexes of glycinin. *J Biol Chem.* 256(16). 8752-5.

Thompson, D., Karpe, F., Lafontan, M., & Frayn, K. (2012). Physical activity and exercise in the regulation of human adipose tissue physiology. *Physiol Rev*. 92(1), 157-191.

Tordjman, J., Guerre-Millo, M., & Clément, K. (2008). Adipose tissue inflammation and liver pathology in human obesity. *Diabetes Metabol*. 34(6), 658-63.

Torre-Villalvazo, I., Tovar, A.R., Ramos-Barragan, V.E., Cerbón-Cervantes, M.A., & Torres, N. (2008). Soy protein ameliorates metabolic abnormalities in liver and adipose tissue of rats fed a high fat diet. *J Nutr*. 138(3), 462-8.

Unger, R.H., & Orci, L. (2000). Lipotoxic diseases of nonadipose tissues in obesity. *Int J Obes Relat Metab Disord.* Nov(24), Suppl 4:S28-32.

Velasquez, M. T., & Bhathena, S. J. (2007). Role of dietary soy protein in obesity. *Int J Med Science*. 4(2), 72-82.

Villares, A., Rostagno, M. A., Garcia-Lafuente, A., Guillamón, E., & Martinez, J. A. (2011). Content and profile of isoflavones in soy-based foods as a function of the production process. *Food Bioprocess Technol*. 4(1), 27-38.

Vincent, A. & Fitzpatrick, L.A. (2000). Soy Isoflavones: Are they useful in menopause? *Mayo Clinic Proceedings*. 74, 1174-84.

Vitale, D. C., Piazza, C., Melilli, B., Drago, F., & Salomone, S. (2013). Isoflavones: Estrogenic activity, biological effect and bioavailability. *Eur J Drug Metab Pharmacokinet*. 38(1), 15-25.

Wang, G., Troendle, M., Reitmeier, C.A., Wang, T. (2012). Using modified soy protein to enhance foaming of egg white protein. *J Sci Food Agri*. 92(10), 2091-7.

Weigle, D.S., Breen, P.A., Matthys, C.C., Callahan, H.S., Meeuws, K.E., Burden, V.R., & Purnell, J.Q. (2005). A high-protein diet induces sustained reductions in appetite, ad libitum caloric intake, and body weight despite compensatory changes in diurnal plasma leptin and ghrelin concentrations. *Am J Clin Nutr.* 82(1), 41-8.

White, U. A., & Tchoukalova, Y. D. (2013). Sex dimorphism and depot differences in adipose tissue function. Biochim Biophys Acta. 1842(3), 377–392.

Wu, Z., Rosen, E. D., Brun, R., Hauser, S., Adelmant, G., Troy, A. E., et al. (1999). Cross-regulation of C/EBPα and PPARγ controls the transcriptional pathway of adipogenesis and insulin sensitivity. *Mol Cell.* 3(2), 151-8.

Xiao, C. W., Wood, C. M., Weber, D., Aziz, S. A., Mehta, R., Griffin, P., & Cockell, K. A. (2014). Dietary supplementation with soy isoflavones or replacement with soy proteins prevents hepatic lipid droplet accumulation and alters expression of genes involved in lipid metabolism in rats. *Genes Nutr*. 9(1), 373.

Xu, H., Barnes, G. T., Yang, Q., Tan, G., Yang, D., Chou, C. J., et al. (2003). Chronic inflammation in fat plays a crucial role in the development of obesity-related insulin resistance. *J Clin Invest.* 112(12), 1821-1830.

Yamauchi, F., Thanh, V.H., Kawase, M., & Shibasaki, K. (1976). Separation of the glycopeptides from soybean 7 S protein: Their amino acid sequences. *Agri Biol Chem*. 40(4), 691-696.

Yamazaki, T., Kishimoto, K., Miura, S., & Ezaki, O. (2012). Dietary β-conglycinin prevents fatty liver induced by a high-fat diet by a decrease in peroxisome proliferator-activated receptor γ protein. *J Nutr Biochem*. 23(2), 123-132.

Yang, X., Belosay, A., Hartman, J.A., Song, H., Zhang, Y., Wang, W., Doerge, D.R., & Helferich, W.G. (2015). Dietary soy isoflavones increase metastasis to lungs in an experimental model of breast cancer with bone micro-tumors. *Clin Exp Metastasis.* 32(4):323-33.

Yang, J., Eliasson, B., Smith, U., Cushman, S.W., & Sherman, A. S. (2012). The size of large adipose cells is a predictor of insulin resistance in first-degree relatives of type 2 diabetic patients. Obesity (Silver Spring). 20(5), 932-8.

Zarkadas, C.G., Gagnon, C., Poysa, V., Khanhizadeh, S., Cober, E.R., Chang, V., & Gleddie, S. (2006). Protein quality and identification of the storage protein subunits of tofu and null soybean genotypes, using amino acid analysis, one- and two-dimensional gel electrophoresis, and tandem mass spectroscopy. *Food Res Int.* 40(1), 111-128.

Zechner, R., Strauss, J., Frank, S., Wagner, E., Hofmann, Kratky, D., Hiden, M., & Levak-Frank, S. (2000). The role of lipoprotein lipase in adipose tissue development and metabolism. *Int J Obes.* 24(Suppl 4), S53-6.

Zhou, D., Lezmi, S., Wang, H., Davis, J., Banz, W., & Chen, H. (2014). Fat accumulation in the liver of obese rats is alleviated by soy protein isolate through β-catenin signaling. *Obesity.* 22(1), 151-8.